# Widely Linear MIMO MMSE Filter and Joint MLSE for VAMOS

by

Wenjie Huang

A thesis
presented to the University of Waterloo
in fulfillment of the
thesis requirement for the degree of
Master of Applied Science
in
Electrical and Computer Engineering

Waterloo, Ontario, Canada, 2010

# AUTHOR'S DECLARATION

I hereby declare that I am the sole author of this thesis. This is a true copy of the thesis, including any required final revisions, as accepted by my examiners.

I understand that my thesis may be made electronically available to the public.

# Abstract

Currently, the 3rd Generation Partnership Project (3GPP) standards body is working actively to specify Voice services over Adaptive Multi-user channels on One Slot (VAMOS), an enhanced transmission scheme to double the voice service capacity in existing Global System for Mobile communications (GSM) system. Capacity increase is achieved by multiplexing two users in the same timeslot within the same radio frequency channel. With this new transmission scheme, several characteristics of VAMOS downlink signals can be taken into account in mobile station equalizer design. Firstly, the base station maps a pair of bits from the two VAMOS users to a quaternary symbol whose I/Q amplitude ratio may vary burst by burst. When the ratio is not unity, the VAMOS downlink signal is improper because its pseudo-covariance does not vanish. Secondly, in the baseband modulation stage, the symbol sequence is processed by $\pi/2$ progressive symbol rotation and linearized Gaussian minimum shift keying (LGMSK) pulse shaping. Hence, intersymbol interference (ISI) is introduced. Lastly, due to tight frequency reuse in most GSM networks today, mobile stations also experience co-channel interference (CCI) from other base stations transmitting various types of signals such as GMSK, 8 phase shift keying (8PSK), or VAMOS. In order to achieve network capacity increase, advanced equalizers in mobile stations are required to offer superior bit error rate (BER) performance in this challenging mobile radio system.

Unlike uplink transmission where a base station is typically equipped with an antenna array to enhance the desired signal and suppress CCI, equalizer design in downlink direction is more challenging because most mobile stations have one antenna only. In the past decade, various single antenna interference cancellation (SAIC) solutions have been developed to mitigate the CCI effect. While these solutions can be straightforwardly reused to obtain acceptable performance in VAMOS, in this work a novel equalizer is proposed to achieve better BER performance by addressing the forementioned characteristics of VAMOS downlink signals. This equalizer consists of a widely linear multiple-input multiple-output (MIMO) minimum mean square error (MMSE) filter and a joint maximum likelihood sequence estimator (JMLSE). In the first stage, since the transmitted signal and the received signal may not be jointly proper, a widely linear filter is more effective in suppressing interference from other base stations plus background noise while preserving the two paired VAMOS users' signal energy. In the next stage, further interference cancellation is achieved by jointly detecting the two users' symbol sequences using JMLSE. Optimality of the proposed equalizer is justified by theoretical proof and simulation in this work.

# Acknowledgements

First of all, I am sincerely grateful to Professor Amir K. Khandani for all of his guidance and inspiration during my graduate program. It was an honor to have an opportunity to develop my academic skills under his supervision. The inspiring discussions helped me overcome academic obstacles, and suggestions to several thesis revisions clarified my understanding of theoretical nuance. A few years ago I was excited to start my study. Now the completion of this program and the guidance from Professor Khandani make me eager to continue my career in wireless communications.

I also would like to thank my thesis readers Professor A. Hamed Majedi and Professor Slim Boumaiza for many corrections they indicated to further improve my work. Additionally, I would like to acknowledge my friend Dr. Dake He for giving me many valuable suggestions and comments.

My greatest appreciation belongs to my wonderful wife Jinli Yin, who took responsibility for most family chores and also emotionally supported me throughout the entire period of my study. In particular, It was an impossible task that she looked after our two lovely but little children without rest in all of those tough times and undertook all daily housework in my last year of study. This work cannot be done without her.

# Dedication

This thesis is dedicated to my beloved wife Jinli Yin, for all of her encouragement, patience, and sacrifices. It is also dedicated to Kevin and Emily, for the joy that they have brought into my life.

# Table of Contents

# List of Figures

# List of Tables

# List of Abbreviations

| | |
|---|---|
| 3GPP | 3rd Generation Partnership Project |
| 8PSK | 8 Phase Shift Keying |
| AWGN | Additive White Gaussian Noise |
| BER | Bit Error Rate |
| BPSK | Binary Phase Shift Keying |
| CCI | Co-Channel Interference |
| CIR | Channel Impulse Response |
| DARP | Downlink Advanced Receiver Performance |
| DFE | Decision Feedback Equalizer |
| FDMA | Frequency Division Multiple Access |
| FER | Frame Error Rate |
| FIR | Finite Impulse Response |
| GMSK | Gaussian Minimum Shift Keying |
| LGMSK | Linearized Gaussian Minimum Shift Keying |
| GSM | Global System for Mobile communications |
| I/Q | In-phase / Quadrature |
| ISI | Intersymbol Interference |
| ITC | Identity Tap Constraint |
| JMLSE | Joint Maximum Likelihood Sequence Estimator |
| MIC | Mono Interference Cancellation |
| MIMO | Multiple-Input Multiple-Output |
| MLSE | Maximum Likelihood Sequence Estimator |

| | |
|---|---|
| MMSE | Minimum Mean Square Error |
| MSE | Mean Square Error |
| MTS | MUROS Test Scenario |
| MUROS | Multi-User Reusing One Slot |
| ONC | Orthonormality Constraint |
| QPSK | Quadrature Phase Shift Keying |
| RSSE | Reduced State Sequence Estimator |
| SAIC | Single Antenna Interference Cancellation |
| SAM | Single Antenna MIMO |
| SCPIR | Sub Channel Power Imbalance Ratio |
| SINR | Interference Plus Noise Ratio |
| TDMA | Time Division Multiple Access |
| TIR | Target Impulse Response |
| TU3 | Typical Urban 3km |
| VAMOS | Voice services over Adaptive Multi-user channels on One Slot |
| VAR | Vector valued Auto-Regressive |
| WLP | Widely Linear Processing |
| WSSUS | Wide Sense Stationary and Uncorrelated Scattering |

# Chapter 1
# Introduction

The past decade has seen stupendous advances in interference cancellation techniques, in both academia and industry. One key practical application is the capacity increase of the Global System for Mobile communications (GSM) system. Although deemed as a second generation (2G) cellular standard comparing with various third generation (3G) and fourth generation (4G) standards, the dominant worldwide coverage of GSM today still drives the industry to integrate advanced wireless communication techniques into products.

GSM is a hybrid frequency division multiple access (FDMA) and time division multiple access (TDMA) cellular system. A user occupies one or a few time slots in a particular frequency channel during a given burst period. When GSM was in use initially, co-channel interference (CCI) was avoided by network configuration because adjacent base stations used different set of radio frequency channels. With the growing demand to increase system capacity, one idea was to use the radio spectrum more frequently across the network, thereby decreasing the so-called frequency reuse factor [1]. When all base stations use the same set of frequencies, the network is said to have reuse factor one. In this scenario, strong CCI presents at the mobile station receive antenna so that interference cancellation capability on the mobile station side is required to support the capacity increase. Unlike base stations which use conventional antenna-array diversity techniques to suppress interference, most mobile stations today have one antenna only. Different single antenna interference cancellation (SAIC) solutions applicable to mobile stations have been proposed since mid 1990s, based on various combinations of linear filtering and non-linear detection algorithms. Using Phillip's Mono Interference Cancellation (MIC) mobile stations, a comprehensive field trial [2] demonstrated 57% network voice service capacity gain in a live network with frequency reuse factor one.

Having seen system capacity gain demonstrated by SAIC-capable mobile stations, participants in the 3rd Generation Partnership Project (3GPP) standards body worked together to standardize performance requirements into 3GPP specifications and introduce SAIC into the mobile handheld market. Since SAIC solutions avoid modification on the base station transmitter side, presumably system capacity can be further increased with a properly designed new transmission scheme. Base on this concept, 3GPP started to work on a new operating mode named Voice services over Adaptive Multi-user channels on One Slot (VAMOS) recently. As of now, the detailed transmission scheme and some simulation results have been documented in the comprehensive 3GPP technical report [3].

Based on this publication as well as other relevant 3GPP documents and IEEE literature, this thesis proposes a novel VAMOS mobile station equalizer offering superior error performance by addressing unique characteristics in the new transmission scheme. Single receive antenna constraint is assumed in this work.

According to [3], VAMOS is based on the existing GSM burst structure but system capacity is doubled by multiplexing two speech users in the same timeslot within the same radio frequency channel. Orthogonal superposition is applied by mapping one user's binary symbol sequence onto the real axis and the other user's binary symbol sequence onto the imaginary axis in the quaternary symbol constellation. This transmission scheme creates two sub-channels for two paired VAMOS users, respectively. In the downlink direction, characteristics relevant to mobile station equalizer design are as follows.

Firstly, an adaptive symbol constellation named α-QPSK is proposed. The quaternary symbol constellation is not necessarily square as in conventional quadrature phase shift keying (QPSK) modulation; that is, the amplitude ratio between the real and imaginary parts of a constellation point may not be unity. This ratio is constant within one burst period but may vary burst by burst. This approach is equivalent to having different downlink transmission power levels in two VAMOS sub-channels in order to facilitate multiplexing mobile stations with different interference cancellation capabilities. More transmission power can be allocated to the sub-channel for the less capable mobile station so that its input signal to interference plus noise ratio (SINR) is stronger. Although the other mobile station experiences weaker input SINR in this case, its advanced interference cancellation capability is able to suppress interference effectively. One consequence of the imbalanced sub-channel transmission power ratio is that the VAMOS transmit signal becomes improper [4]; that is, its pseudo-covariance (covariance of the signal with its complex conjugate version) does not vanish. It is found in [5, 6] that when the input signal is improper, widely linear filters may yield smaller output mean square error (MSE) than their linear counterparts.

Secondly, to support legacy GSM mobile stations which assume that the desired user signal is Gaussian minimum shift keying (GMSK), in VAMOS the symbol sequence is processed by symbol-by-symbol $\pi/2$ phase rotation and linearized GMSK (LGMSK) pulse shaping in the baseband modulator. The LGMSK pulse spans 3 symbol periods approximately; hence, inter-symbol interference (ISI) is introduced. This modulation scheme generates a near-GMSK signal [7] so that compatibility with existing mobile stations is maintained. On the receiver side, most receivers

perform $\pi/2$ phase derotation before equalization. The cascade of the $\pi/2$ phase rotation and LGMSK pulse shaping at the transmitter, the multipath fading channel, and the $\pi/2$ phase derotation at the receiver creates an equivalent linear complex-valued ISI channel from the equalizer's perspective. Since the corresponding CIR coefficients consist of different complex values, a simple preprocessing method on the receiver side such as sample-wise projection (projecting the received samples into some direction in the complex plane) cannot suppress the paired VAMOS user's signal effectively, although the VAMOS sub-channels are orthogonal before baseband modulation on the transmitter side. The desired user's signal is interfered by the paired user's signal in a similar fashion as CCI.

In addition to the unique VAMOS transmission characteristics as above, mobile stations in VAMOS mode also need to deal with CCI generated from other base stations. The interfering signals can be GMSK which is always improper, 8 phase shift keying (8PSK) which is always proper, or VAMOS which may or may not be proper depending on the sub-channel transmission power ratio. In a dense urban environment, it is common for a mobile station to receive multiple interfering signals of different modulation types at various power levels. In the problem formulation for equalizer design, disturbance in a dense urban area (where VAMOS is mainly in use) can be modeled as interference plus additive white Gaussian noise (AWGN). The interference consists of one or several co-channel signals from other base stations and the AWGN part mainly contains receiver thermal and quantization noise.

Numerous interference cancellation solutions applicable to mobile station equalizer design have been proposed in recent years. They can be classified into the following three categories.

Equalizers in the first category consist of two major components, a linear or widely linear filter and a maximum likelihood sequence estimator (MLSE). The filters in most solutions are designed to enhance the desired signal and suppress the interference plus noise in general, but have different design criteria. In [8], the filter coefficients and the post-filter target impulse response (TIR) (or modified channel vector as in [8]) are jointly optimized to maximize the output SINR. In [9, 10], MMSE filters are used to minimize the output MSE. Noise whitening filters were also applied by some authors, such as in [11]. Some other proposals reduce equalizer computation complexity, such as the one in [12]. This solution does not perform computation intensive eigendecomposition and matrix inversion. It is sub-optimum in interference plus noise scenarios because the filter is designed to cancel the dominant interferer. In the last few years, widely linear process has been applied in many publications to further improve output SINR in the improper transmitted signal or improper

received signal cases. A recent widely linear filter based MLSE equalizer can be found in [13]. In the second stage of equalization, a single-user MLSE is used to detect the desired user's symbol sequence. Many solutions assume that the residue disturbance is AWGN and use MLSE directly in this stage. [8] suggested to place a noise whitening filter before MLSE and demonstrated 1 dB error performance gain by simulation. Instead of using a conventional Euclidean metric Forney-type MLSE [14], if a minimum phase filter is included such as in [11, 13], a reduced state sequence estimator (RSSE) [15] also offers near-optimum BER performance but computation complexity can be reduced significantly.

The second category of equalizers is named multiuser detection or joint detection by some authors, because the desired user and interfering users' sequences are detected simultaneously. Joint maximum likelihood sequence estimator (JMLSE) is one of the most effective algorithms used in multiuser detection. This algorithm was originally proposed in [16], and probably first applied in GSM by [17]. When the CIR of the desired user and all interferers are known to the equalizer, multiuser detection typically offers better performance than filter based solutions. However, several issues prevent easy application of multiuser detection in practice. When CIR needs to be estimated or symbol constellations have to be blindly detected, multiuser detection's error performance may degrade drastically. Meanwhile, when the number of users or the sizes of some symbol constellations are large, the computation complexity is high and also the error performance degrades (due to reduced minimum Euclidean distance between two valid transmitted sequences). For computation complexity reduction, many authors have suggested different pre-filters to reduce the number of trellis states for JMLSE, such as the maximum SINR channel shortening prefilter [18] and the minimum phase MIMO prefilter [19].

Naturally, the third category is a hybrid of the two forementioned categories, typically consisting of a MIMO filter in the first stage and a JMLSE in the second stage. In the filtering stage, the desired user's signal and a few dominant interfering signals are deemed as wanted signals, and other signals are considered disturbance. The filter is designed to maximize the output SINR between the wanted signals and disturbance. In the next JMLSE stage, sequences of the desired and dominant interfering users are detected jointly. In VAMOS, we may deem signals from the two paired VAMOS users as wanted signals and other signals as disturbance. This is a practical approach because training sequences and symbol constellations of the two paired VAMOS users are known to the mobile station, but those values of the interfering users from other base stations have to be blindly detected.

The idea has been utilized in [20] to design a VAMOS equalizer dubbed single antenna MIMO (SAM) receiver. In that solution, the overall channel is deemed as a 2-input (denoting the two paired VAMOS users transmitting binary symbol sequences) and 2-output (denoting the real and imaginary parts of the received temporal samples from the single mobile station antenna) real-valued channel matrix; and, the interference plus noise is modeled as a vector valued auto-regressive (VAR) process [21]. Hence, the equalizer is a straightforward extension of the spatio-temporal interference rejection algorithm in [21]. To be specific, in the first stage, with a VAR model to approximate interference plus noise, a finite impulse response (FIR) filter with the same order whitens the spatially and temporally correlated disturbance in the received samples. In the second stage, a conventional two-user JMLSE detects the two VAMOS binary symbol sequences jointly.

The equalizer proposed in this work belongs to the third category. It is similar to the SAM receiver above in two aspects. Firstly, we also have two-stage processing where the first stage is a filter and the second stage is a JMLSE. Secondly, we treat the two paired VAMOS signals as wanted signals and the remaining interference plus noise as disturbance.

However, the filter design in our proposal is different. It consists of a reduced-rank widely linear MIMO MMSE filter and a CIR correction and noise balance unit. To be specific, rank reduction is used to compensate for inaccurate estimates of second order statistics; this is a scalable approach and can be straightforwardly extended to the full rank form when accurate second order statistics are available (such as in a high input SINR scenario). Widely linear processing is applied to take into account that transmitted signals or received signals may be improper. MIMO filter structure is used to process the augmented input vector formed by stacking spatial and temporally adjacent samples, a technique named space-time data model [8]. The filter coefficient matrix is computed by jointly optimizing it and the TIR to minimize the filter output MSE. MMSE instead of a noise whitening algorithm is preferred because computation of MMSE filter coefficients uses the more accurately estimated autocorrelation matrix of the received sample vector (which can be estimated directly based on received samples) but whitening noise requires the autocorrelation matrix of the noise vector (which is indirect to estimate because noise samples are not received directly). Moreover, since the actual overall CIR after the MMSE filter output differs from TIR and the noise power at different filter output taps are unequal, a CIR correction and noise balance unit is designed to process the filter outputs before the next JMLSE stage.

## 1.1 Contributions of the thesis

This work describes a novel VAMOS equalizer consisting of a reduced-rank widely-linear MIMO MMSE filter, a CIR correction and noise balance unit, and JMLSE. Proof will be derived to justify the exact equivalence between this equalizer and noise whitening filter based MLSE equalizers when second order statistics are known. Since in correlated Gaussian noise situation an equalizer consisting of a noise whitening filter and JMLSE is optimum [16, 22], the proposed MMSE filter based equalizer is optimum as well. The advantage of MMSE filters instead of noise whitening filters lies in coping with inaccurate estimates of second order statistics as we have just mentioned above. In the simulation part, besides confirming the equivalence of the two types of equalizers in both noise-limited and interference-limited test scenarios, we also demonstrate the performance gain of the proposed equalizer w.r.t. other equalizers in various VAMOS test scenarios.

Besides, a comprehensive literature survey is documented to describe recent years' advances in the interference cancellation research area. Some insightful analysis will be provided to elaborate differences and similarities among some solutions.

## 1.2 Organization of the thesis

To describe problem formulation in detail, chapter 2 depicts the baseband transmitter, the receiver, the frequency-selective multipath fading model, and the interference models in VAMOS operating mode.

Chapter 3 contains a literature survey of recent years' interference cancellation algorithms. It consists of three sections corresponding to the forementioned three categories of interference cancellation solutions, respectively.

In chapter 4, we describe the proposed equalization algorithm in detail and prove its equivalence to the noise whitening filter based equalizer.

Comprehensive simulation work is documented in chapter 5. Some simulation plots confirm the theoretical analysis in chapter 4 and others are used to find the performance gain of our proposal w.r.t. other equalizers.

Finally, we summarize the conclusions and list remaining issues to investigate in chapter 6.

# Chapter 2

# Discrete-time baseband transmission model in VAMOS

In this chapter, in order to clarify the problem formulation in some detail, the following four sections describe the transmitter, the receiver, the multipath fading channel model, and the VAMOS interference test scenarios, respectively. A diagram below depicts the overall discrete-time baseband transmission model in VAMOS operating mode.

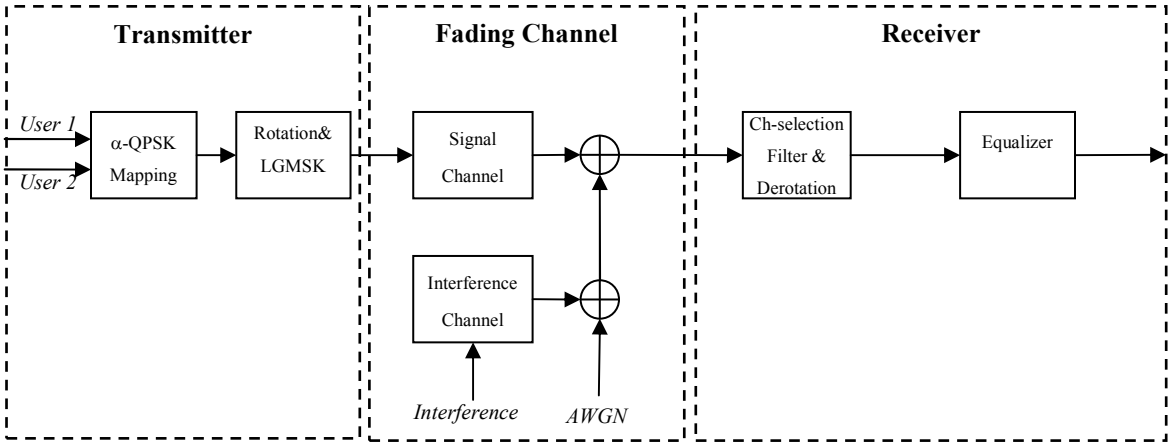


**Figure 2.1 The discrete-time baseband transmission model**

## 2.1 The baseband transmitter structure

Two main processing units in the baseband transmitter, α-QPSK symbol constellation mapping and Rotation & linearized GMSK (LGMSK) pulse shaping, are described below, followed by the VAMOS burst structure elaborated in the last subsection.

### 2.1.1 $\alpha$-QPSK symbol constellation mapping

This unit assigns two bits from the two VAMOS users, respectively, to a quaternary symbol whose amplitude ratio may vary burst by burst. Hence, the symbol constellation may not be square [3]. The ratio of the amplitudes of real and imaginary parts (representing the ratio of the amplitudes of the two users) is controlled by α, where $0 \leq \alpha \leq \sqrt{2}$. When α=1, the two users are transmitted with the same power level and the constellation is the same as the conventional QPSK. When $1 < \alpha \leq \sqrt{2}$, the downlink signal of the first user is transmitted with higher power. When $0 \leq \alpha < 1$, the downlink

signal of the second user is transmitted with higher power. The mapping between a constellation point and a pair of bits from the two users is mathematically expressed as follows [3]

$$\alpha\sqrt{\frac{1}{2}}+\mathrm{j}\sqrt{2-\alpha^2}\sqrt{\frac{1}{2}},\ \text{when user } 1,2=(1,1) \tag{2.1}$$

$$\alpha\sqrt{\frac{1}{2}}-\mathrm{j}\sqrt{2-\alpha^2}\sqrt{\frac{1}{2}},\ \text{when user } 1,2=(1,0) \tag{2.2}$$

$$-\alpha\sqrt{\frac{1}{2}}+\mathrm{j}\sqrt{2-\alpha^2}\sqrt{\frac{1}{2}},\ \text{when user } 1,2=(0,1) \tag{2.3}$$

$$-\alpha\sqrt{\frac{1}{2}}-\mathrm{j}\sqrt{2-\alpha^2}\sqrt{\frac{1}{2}},\ \text{when user } 1,2=(0,0) \tag{2.4}$$

The introduction of the $\alpha$ value is intended to facilitate pairing mobile stations with different interference cancellation capabilities. More power can be allocated to the sub-channel for the less capable mobile station to increase its input SINR. Although input SINR for the more capable mobile station is reduced, its advanced interference cancellation capability can improve the error performance effectively.

when $\alpha$=1, the symbol constellation is square and the VAMOS signal is proper [4] because its pseudo-covariance vanishes; otherwise, the constellation is rectangular and the signal is improper because its pseudo-covariance does not vanish. This can be seen by the derivation of the pseudo-covariance of a VAMOS signal $x = x_R + x_I j$ as below.

$$\mathrm{E}[xx] = \mathrm{E}[(x_R + x_I j)(x_R + x_I j)] = \mathrm{E}\left[x_R^2 - x_I^2\right] + 2j\mathrm{E}[x_R x_I] = \mathrm{E}\left[x_R^2\right] - \mathrm{E}\left[x_I^2\right] \tag{2.5}$$

In the last conversion we have assumed that $x_R$ and $x_I$ are independent and zero-mean. When $\alpha$=1, $x_R$ and $x_I$ are identically distributed so that the pseudo-covariance vanishes; otherwise, the pseudo-covariance is a non-zero value and widely linear filters [5, 6] may offer performance gain.

### 2.1.2 Rotation & LGMSK pulse shaping

Symbol by symbol $\pi/2$ phase rotation and LGMSK pulse shaping together contribute to the compatibility to the conventional GMSK system.

VAMOS is designed to reuse the GSM system. Hence, the symbol rate is 270.833 KHz and the channel spacing in frequency domain is still 200 KHz, as in GSM standard. To ensure legacy GSM mobile stations able to be multiplexed in VAMOS mode, the downlink signal on its subchannel

should resemble a standard GMSK signal. The solution provided in [3] is symbol by symbol $\pi/2$ phase rotation followed by LGMSK pulse shaping.

It was proved In [7] that the conventional GSM signal (the cascade of differentially encoding a binary symbol sequence, followed by GMSK phase modulation) can be exactly represented by passing a sequence $j^{k+1}a_k$ (progressive $\pi/2$ phase rotation of a binary symbol sequence $a_k$) through a pulse shaping filter, in which the pulse consists of a set of impulses $C_N(t)$ weighed by the past L data values $a_{k-1}, \ldots, a_{k-L}$

$$\underline{e}(t) = \sum_{K=0}^{\infty} j^{k+1} a_k \cdot \sum_{N=0}^{2^{L-1}-1} \exp\left(-j\frac{\pi}{2}\sum_{l=1}^{L-1}\alpha_{N,l}\right) \cdot \prod_{l=1}^{L-1}(a_{k-l-1}a_{k-l})^{\alpha_{N,l}} \cdot C_N(t-kT) \qquad (2.6)$$

where $\underline{e}(t)$ is the complex envelope at the pulse shaping filter output. The exact expression of $\alpha_{N,l}$ and $C_N(t)$ in [7] is omitted for simplicity.

Figure 2.2 duplicated from [7] reveals the fact that the first impulse $C_0(t)$ contains much more energy than other impulses $C_N(t)$, according to the amplitude values in these plots.

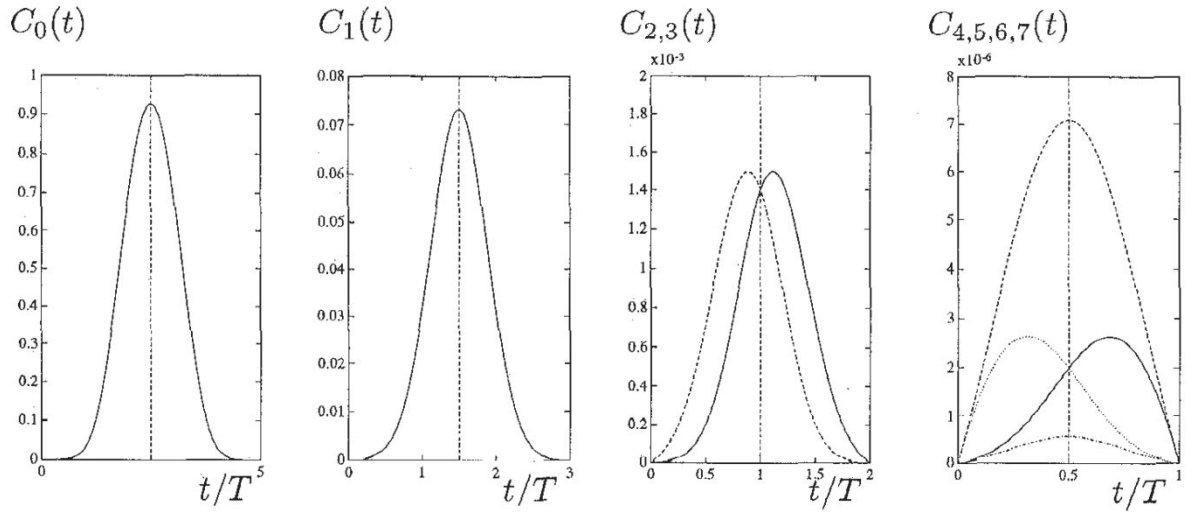


**Figure 2.2 Impulses of GMSK with time-bandwidth product 0.3 and L=4, duplicated from** [7]

Hence, it is obvious that with the same input binary symbol sequence, if one output is produced by differential encoding followed by standard GMSK phase modulation and another output is produced by $\pi/2$ phase rotation followed by pulse shaping with $C_0(t)$, the two outputs should look similar (but not the same because the pulse shaping filter does not use impulses other than $C_0(t)$). From the plot of $C_0(t)$, it is apparent that most signal energy of $C_0(t)$ is limited within 3 symbol periods.

### 2.1.3 The VAMOS burst structure

A diagram below shows the standard GSM burst structure according to 3GPP GSM specification [23]. VAMOS uses the same burst structure.

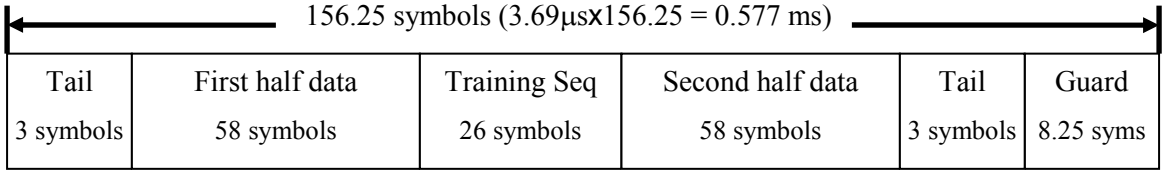


**Figure 2.3 Standard GSM burst structure**

In the diagram, we see that the 26 training sequence symbols are in the middle of the burst, and three known tail symbols exist at both ends, respectively. This structure facilitates backward sequence detection for the first half data. That is, we detect the "first half data" by backward sequence detection, with the starting trellis state defined by the first several training symbols and the ending state constrained by the three tail symbols in the beginning of the burst.

## 2.2 The receiver front-end structure

Before baseband signal processing, a typical receiver front-end may consist of a homodyne RF receiver (to down convert the RF signal to baseband), a high-speed sigma-delta modulator plus a decimation filter (to quantize the analog signal into oversampled I/Q samples), and several digital channel selection filters (to preserve the in-band signal energy but suppress the out-band signal energy) [24]. At the input of the baseband signal processing unit are baseband I/Q samples, possibly oversampled.

Before equalization or probably considered as the initial step of equalization, progressive symbol-by-symbol $\pi/2$ phase de-rotation is performed to create an equivalent linear complex-valued overall channel from the equalizer's perspective. In particular, if one sample is taken per symbol period (no oversampling), the complex-valued I/Q sample at sample index n is multiplied by $e^{-j(n*\pi/2)}$; if two samples are taken per symbol period (2x oversampling), the I/Q sample at sample index n is multiplied by $e^{-j(n*\pi/4)}$.

## 2.3 The frequency-selective multipath fading model adopted by VAMOS

In an urban area where VAMOS is mainly in use, a mobile station is typically near the ground and surrounded by many nearby scatterers; hence, the downlink channel is a rich-scattering multipath fading channel. Moreover, since the delay spread of the typical urban fading profile defined in annex C.3 of [25] is comparable to one symbol period, different frequency components in the transmitted signal experience different attenuation; hence a frequency-selective fading effect occurs.

Although many waves travel from the transmitter to the receiver at a given time, they can be grouped into different paths according to their propagation delays. The resulting channel can be modeled as a transversal filter with tap spacing $\Delta\tau$ and time-varying tap gains $c(t, m\Delta\tau)$ as expressed in [26]

$$r(t) = \sum_{m=0}^{n} u(t - \Delta\tau)c(t, m\Delta\tau)\Delta\tau \quad (2.7)$$

where $r(t)$ is the received signal, $c(t, m\Delta\tau)$ is the time-varying CIR function, and $u(t)$ is the transmitted signal.

VAMOS adopts the same multipath fading profiles used in GSM. As described in 3GPP GSM specification [25], the radio channel model is wide sense stationary and uncorrelated scattering (WSSUS) [26], where *widely sense stationary* refers to the fact that the autocorrelation of the CIR function in each path depends on time difference instead of t and *uncorrelated scattering* means that paths with different delays are uncorrelated.

Various multipath fading profiles applicable to various radio environments are specified in [25]. The typical urban fading profile with 12 taps is given in the table below, in which two equivalent alternative tap settings are specified. In this table, the classical Doppler power spectrum, dubbed CLASS, specifies the simulation model of amplitude variation w.r.t. the mobile station moving speed.

| Tap Number | Relative time (us) | | Average relative power (dB) | | Doppler spectrum |
|---|---|---|---|---|---|
| | (1) | (2) | (1) | (2) | |
| 1 | 0.0 | 0.0 | -4.0 | -4.0 | CLASS |
| 2 | 0.1 | 0.2 | -3.0 | -3.0 | CLASS |
| 3 | 0.3 | 0.4 | 0.0 | 0.0 | CLASS |
| 4 | 0.5 | 0.6 | -2.6 | -2.0 | CLASS |

| | | | | | |
|---|---|---|---|---|---|
| 5 | 0.8 | 0.8 | -3.0 | -3.0 | CLASS |
| 6 | 1.1 | 1.2 | -5.0 | -5.0 | CLASS |
| 7 | 1.3 | 1.4 | -7.0 | -7.0 | CLASS |
| 8 | 1.7 | 1.8 | -5.0 | -5.0 | CLASS |
| 9 | 2.3 | 2.4 | -6.5 | -6.0 | CLASS |
| 10 | 3.1 | 3.0 | -8.6 | -9 | CLASS |
| 11 | 3.2 | 3.2 | -11.0 | -11.0 | CLASS |
| 12 | 5.0 | 5.0 | -10.0 | -10.0 | CLASS |

**Table 2.1 Fading profile for typical urban environment (12 tap setting), duplicated from** [25]

From the table it can be seen that most of the energy of the delay taps is concentrated within one symbol period (3.69 μs). Since the LGMSK pulse $C_0(t)$ in the transmitter spans 3 symbol periods approximately, the equivalent overall channel spans four symbol periods.

## 2.4 The VAMOS interference test scenarios

Besides multipath fading profiles, specification of the interference test scenarios is also necessary to complete the problem formulation. In annex L of the 3GPP GSM specification [25], several interference test scenarios were specified for Downlink Advanced Receiver Performance (DARP) capable mobile stations. DARP is the 3GPP equivalent name of SAIC, and it is the predecessor of VAMOS. In that 3GPP specification, interferers in all test scenarios are GMSK-modulated signals. The main differences among various test scenarios are the number of interferers, their relative power levels, whether interferers are burst-wise synchronized with the desired user's signal, and whether AWGN is included. In 3GPP VAMOS technical report [3], these interference test scenarios were reused but each scenario can have either GMSK or VAMOS interferers. We summarize different VAMOS test scenarios into a table, by consolidating various tables in section 5.2 of [3]. MTS in this table is the abbreviation of Multi-User Reusing One Slot (MUROS) test scenarios. MUROS and VAMOS are interchangeable in most 3GPP publications.

| Reference Test Scenario | Interfering Signal | Interferer Relative Power Level | Training Sequence Code | Interferer Delay |
|---|---|---|---|---|
| MTS-1 | Co-channel 1 | 0 dB | None | No delay |
| MTS-2 | Co-channel 1 | 0 dB | None | No delay |

| | | | | |
|---|---|---|---|---|
| | Co-channel 2<br>Adjacent 1<br>AWGN | -10 dB<br>3 dB<br>-17 dB | None<br>None<br>- | No delay<br>No delay<br>- |
| MTS-3 | Co-channel 1 | 0 dB | None | 74 symbols |
| MTS-4 | Co-channel 1<br>Co-channel 2<br>Adjacent 1<br>AWGN | 0 dB<br>-10 dB<br>3 dB<br>-17 dB | None<br>None<br>None<br>- | 74 symbols<br>No delay<br>No delay<br>- |

**Table 2.2 VAMOS interference test scenarios**

The equalizer proposed in this work considers both interference and noise. To reduce the number of test scenarios in performance evaluation, a noise-limited scenario and an interference-limited scenario are tested in the simulation. In the noise-limited scenario, the disturbance is only AWGN noise; while in the interference-limited scenario, the disturbance consists of a VAMOS interfering signal with various $\alpha$ values and a -15 dB (w.r.t. the power of the desired signal) AWGN noise. This interference-limited test scenario is close to the practical situation because in a frequency-hopping network a mobile station may experience only one dominant interferer from an adjacent base station at a time as well as much weaker interferers from non-adjacent base stations plus receiver internal noise.

# Chapter 3
# Current interference cancellation solutions

Interference cancellation (or suppression, rejection, etc.) in radio transmission has been an active research area in the past 50 years. Numerous solutions based on linear filters, non-linear detectors and combinations of filtering and detection algorithms were proposed. For practical mobile station equalizers, besides the general BER performance criterion, one or several following requirements are required. The solution has to be computation efficient; it is insensitive to inaccurate channel estimation; and, it is expected to adaptively reject various types of interfering signals.

In this chapter, the survey of existing interference cancellation literature includes three sections, corresponding to the three categories of interference cancellation solutions described in the introduction chapter. Some insightful comparisons are provided to elaborate the differences and similarities among some solutions.

## 3.1 Equalizers consisting of (widely) linear filtering and single user MLSE

The first category of interference cancellation equalizers uses a linear or widely linear filter to suppress CCI in the received signal first, followed by a single-user non-linear sequence detector such as MLSE to detect the desired user's symbol sequence. Most of the differences among these solutions lie in the filter design while a conventional MLSE [14] or its reduced-complexity counterpart such as reduced state sequence estimator (RSSE) [15] is used in the sequence detection stage.

Most filters in these solutions are based on some classical filtering techniques. Their commonality is briefed as follows. Firstly, the standard multiple-input spatial filter structure can be used in a single-antenna mobile station by building an augmented received sample vector. In particular, the oversampled received signals during one symbol period can be considered from different channels [27]; received signals and their complex conjugate version can be considered as independent signals to be processed by a widely linear filter [5]; the received sample vector can be further augmented by stacking samples belonging to adjacent symbol periods, an approach named space-time data model [8]. In the text below, we refer to these concepts as multiple-virtual-antenna or multiple-virtual-channel solutions. Secondly, with an augmented received sample vector as input and using the spatial filter structure, application of the classical filtering algorithms such as MMSE [28], maximum SINR [29], or minimum output energy [30] filters becomes relatively straightforward. Thirdly, some solutions used rank-reduction technique. In particular, the M-input N-output channel matrix is

approximated by a rank-r matrix with r<min(M,N). As a result, the MIMO interference cancellation filter matrix has the same rank r, either in a N-input N-output MIMO form or without losing information in an N-input r-output form. Finally, between the interference cancellation filter and MLSE, some solutions include a trellis-state-reduction and/or noise whitening MLSE prefilter based on classical channel shortening filter [31] or minimum-phase noise-whitening filter [32].

Several solutions related to our work are described in the following subsections.

### 3.1.1 Full-rank and reduced-rank space-time equalization

[33] described the full-rank and reduced-rank channel matrix based equalization in the spatially correlated disturbance situation. The noise whitening filter plus MLSE equalizer in that publication is optimum in the sense that the BER performance is the best among all equalizers. This is due to the fact that the noise whitening filter is an invertible operation and MLSE is the optimum approach in dealing with signals disturbed by ISI and AWGN, which is the situation at the noise whitening filter output.

Define $q^{-1}$ as the unit delay operator and assume the receiver antenna array has multiple sensors and the overall CIR $\mathbf{b}(q^{-1})$ has L temporal taps, the received sample vector is

$$x(t) = \mathbf{b}(q^{-1})d(t) + \mathbf{n}(t) = (b_0 + \cdots + b_{L-1}q^{-L+1})d(t) + \mathbf{n}(t) \tag{3.1}$$

where d(t) is the transmitted symbol, and $\mathbf{n}(t)$ is the disturbance consisting of interference plus noise.

The author ignored temporal correlation in the disturbance and approximated it as spatially correlated only with spatial covariance matrix $\mathbf{R}_{nn} = E[\mathbf{n}(t)\mathbf{n}^H(t)]$. Without losing information, $\mathbf{x}(t)$ is filtered with a noise-whitening filter $\mathbf{R}_{nn}^{-1/2}$ and the overall CIR becomes $\mathbf{b}'(q^{-1}) = \mathbf{R}_{nn}^{-1/2}\mathbf{b}(q^{-1})$. In this case, one optimum solution can be the cascade of a conventional multi-channel matched filter and Ungerboeck-type MLSE [34], as used by the author. The multi-channel matched filter can be expressed as

$$\mathbf{w}(q) = \mathbf{b}^H(q)\mathbf{R}_{nn}^{-1} = \mathbf{b}'^H(q)\mathbf{R}_{nn}^{-1/2} \tag{3.2}$$

When the channel $\mathbf{b}$ is known to be low rank, reduced-rank multi-channel matched filter is expected to offer better performance, because it is less sensitive to inaccurate channel estimation than the full-rank filter.

$\mathbf{b}'(q^{-1})$ is a length-M vector (assuming M antenna sensors) and its entries are L-order polynomials representing the temporal delay spread seen by each antenna sensor. Convert it into M-by-L matrix form, we have $\mathbf{B}' = [\mathbf{b}'_0\ \mathbf{b}'_1 \dots \mathbf{b}'_{L-1}]$. It can be decomposed into $\mathbf{B}' = \mathbf{U}\mathbf{V}^H$, where $\mathbf{U} = [\mathbf{u}_1\ \mathbf{u}_2 \dots \mathbf{u}_K]$, $\mathbf{V} = [\mathbf{v}_1\ \mathbf{v}_2 \dots \mathbf{v}_K]$ and K=min(M,L). Here we arrange the vectors in $\mathbf{V}$ according to the order $\|\mathbf{v}_1\| \geq \|\mathbf{v}_2\| \geq \cdots \geq \|\mathbf{v}_K\|$. Then, we know that if $\mathbf{B}'$ is rank $K_r$<K, only the first $K_r$ vectors in $\mathbf{V}$ is non-zero and $\mathbf{B}'$ can be perfectly reconstructed by $[\mathbf{u}_1\ \mathbf{u}_2 \dots \mathbf{u}_{K_r}][\mathbf{v}_1\ \mathbf{v}_2 \dots \mathbf{v}_{K_r}]^H$.

Using the decomposition results above and the equivalence between vector expression $\mathbf{v}_k$ and polynomial expression $v_k(q^{-1})=v_{k,0}+v_{k,1}q^{-1}+\dots+v_{k,L-1}\,q^{L-1}$, the reduced-rank $\mathbf{b}'(q^{-1})$ is

$$\mathbf{b}'(q^{-1}) = \sum_{k=1}^{K_r} \mathbf{u}_k \mathbf{v}_k(q^{-1}) \tag{3.3}$$

The corresponding multi-channel matched filter is

$$\mathbf{w}(q) = \mathbf{b}'^H(q)\mathbf{R}_{nn}^{-1/2} = \sum_{k=1}^{K_r} v_k^H(q)\mathbf{u}_k^H\mathbf{R}_{nn}^{-1/2} \tag{3.4}$$

The overall reduced-rank multi-channel filter operation, including the noise-whitening filter $\mathbf{R}_{nn}^{-1/2}$, can be expressed as

$$z(t) = \mathbf{w}(q)\mathbf{x}(t) = \sum_{k=1}^{K_r} v_k^H(q)\,\mathbf{u}_k^H\mathbf{R}_{nn}^{-1/2}\mathbf{x}(t) = \sum_{k=1}^{K_r} v_k^H(q)\,\tilde{\mathbf{u}}_k^H\mathbf{x}(t) \tag{3.5}$$

where $\tilde{\mathbf{u}}_{k=}\mathbf{R}_{nn}^{-1/2}\mathbf{u}_k$ can be considered as the k-th spatial beamformer.

### 3.1.2 Rank-1 space-time equalization with space-time data model

This subsection describes another solution in [8]. It is directly related to single-antenna mobile stations because it has introduced a space-time data model to augment the received sample vector, making interference cancellation filter more effective. A two-stage interference cancellation equalizer was proposed. The first stage is a MISO space-time filter designed to maximize SINR for the desired user. The second stage is a conventional scalar-input MLSE.

The received sample vector in [8] can be expressed as

$$\mathbf{x}_k = \sum_{j=0}^{v} \mathbf{h}_j s_{k-j} + \sum_{j=0}^{u} \mathbf{c}_j z_{k-j} + \mathbf{n}_k = \mathbf{H}\mathbf{s}_k + \mathbf{C}\mathbf{z}_k + \mathbf{n}_k \tag{3.6}$$

where $\mathbf{h}_j$ is the j-th spatial signature of the desired user's CIR channel matrix $\mathbf{H}$, $\mathbf{c}_j$ is the j-th spatial signature of the interferer's CIR channel matrix $\mathbf{C}$, and $\mathbf{n}_k$ is AWGN. By stacking L+1 temporally adjacent received sample vectors, we create a space-time data model

$$\overline{\mathbf{x}}_k = \overline{\mathbf{H}}\overline{\mathbf{s}}_k + \overline{\mathbf{C}}\overline{\mathbf{z}}_k + \overline{\mathbf{n}}_k \tag{3.7}$$

where $\overline{\mathbf{s}}_k = [s_k, \dots, s_{k-v-L}]^T, \overline{\mathbf{z}}_k = [z_k, \dots, z_{k-u-L}]^T, \overline{\mathbf{n}}_k = [\mathbf{n}_k^T, \dots, \mathbf{n}_{k-L}^T]^T$, and $\overline{\mathbf{H}}$ and $\overline{\mathbf{C}}$ are block Toeplitz matrices built based on **H** and **C**, respectively.

Two filter optimization algorithms were given to jointly optimize the filter coefficient vector of the MISO filter **w** and the post-filter overall CIR **h**. One is based on the least square sense by using the data matrix directly. The other is based on second-order statistics sense. Both methods give the same result so that we describe the one based on second-order statistics sense.

The objective is to maximize the following filter output SINR function.

$$\max_{w,h} \frac{E\left\|\mathbf{h}^T\overline{\mathbf{s}}_k\right\|^2}{E\left\|\mathbf{w}^T\overline{\mathbf{x}}_k - \mathbf{h}^T\overline{\mathbf{s}}_k\right\|^2} \tag{3.8}$$

Since there is no loss to constrain **h** with unit norm, the equivalent approach is to minimize the denominator

$$E\left\|\mathbf{w}^T\overline{\mathbf{x}}_k - \mathbf{h}^T\overline{\mathbf{s}}_k\right\|^2 \tag{3.9}$$

This optimization is a standard MMSE problem. By substituting $\mathbf{w}_{opt} = \sigma_s^2\mathbf{R}_{\overline{\mathbf{x}}}^{-1}\overline{\mathbf{H}}^*\mathbf{h}_{opt}$ (where $\sigma_s^2 = E[s_k s_k^*]$) into $\left\|\mathbf{w}^T\overline{\mathbf{x}}_k - \mathbf{h}^T\overline{\mathbf{s}}_k\right\|^2$, we then find $\mathbf{h}_{opt}$ as the eigenvector corresponding to the smallest eigenvalue of $\mathbf{I} - \sigma_s^2\overline{\mathbf{H}}^T\mathbf{R}_{\overline{\mathbf{x}}}^{-1}\overline{\mathbf{H}}^*$.

### 3.1.3 Spatio-temporal interference rejection combining filter

Previous solutions deem the disturbance as unstructured spatially and/or temporally correlated Gaussian noise. In [21], disturbance **n**(t) is modeled as a K-th order vector-valued autoregressive (VAR) Gaussian process specified by the AR coefficient matrix **A**=[$\mathbf{A}_1$ … $\mathbf{A}_K$ ] and driven by a spatially correlated Gaussian noise **e**(t) with autocorrelation matrix $E[\mathbf{e}(t)\mathbf{e}^H(s)] = \mathbf{Q}\delta_{t,s}$, expressed as below

$$\mathbf{n}(t) = \sum_{k=1}^{K}\mathbf{A}_k\mathbf{n}(t-k) + \mathbf{e}(t) \tag{3.10}$$

This model facilitates the design of the noise whitening filter, which is the prefilter for MLSE in the spatially and temporally correlated noise scenario [11, 33]. We know the fact that although in reality the interference is generally a moving average (MA) process due to the overall CIR of the interferer, a high-order VAR process is able to approximate a MA process reasonably. For the design

of the noise whitening filter, if the disturbance can be modeled as a VAR process, the filter to whiten a K-th order VAR process specified by **A** and **Q** above is an K-th order FIR filter with the filter coefficient matrix $\mathbf{Q}^{1/2}[\mathbf{I} \ -\mathbf{A}]$.

Two issues constrain the FIR filter order K to be a small value and thereby make the solution suboptimum. Firstly, filtering the received samples with a K-order FIR filter increases the overall CIR length by K-1; hence, the MLSE computation complexity increases with a large K. Secondly, in practice such as GSM or VAMOS, **A** and **Q** have to be estimated based on 26 training symbols. A larger K value makes the estimates of **A** and **Q** very inaccurate. However, we know that a small K value causes the VAR model to be considerably different from the actual interference. Simulation in a more recent publication [11] found that spatio-temporal block decorrelation (STBD) noise whitening filter yielded better BER performance than this VAR model based noise whitening filter. In that simulation, K was selected as 2 (the author in [11] denoted it as M=1 equivalently).

### 3.1.4 Full-rank space-time equalization by decorrelation of correlated disturbance

[11] proposed a spatio-temporal block decorrelation (STBD) equalizer. This recent publication is also suitable for single-antenna equalization.

Consider the following transmission model

$$\mathbf{r}[n + n_0] = \sum_{k=0}^{L} \mathbf{c}[k]s[n - k] + \mathbf{v}[n] \tag{3.11}$$

where $\mathbf{c}[k]$ is the length-$n_r$ k-th spatial signature of the length-L CIR matrix, s[n] is the transmitted symbol, $\mathbf{v}[n]$ is the noise vector, and $\mathbf{r}[n]$ is the received sample vector possibly consisting of outputs from multiple receive antennas, separated I and Q components of a complex-valued sample, and oversampling.

With essentially the same space-time data model as [8], by vertically stacking (M+1) temporally adjacent received sample vectors, a spatio-temporally stacked signal model can be expressed as

$$\begin{aligned} \mathbf{r}_M[n + n_0] &\triangleq \mathrm{vec}\big([\mathbf{r}[n], \mathbf{r}[n-1], \dots, \mathbf{r}[n-M]]\big) \\ &= \boldsymbol{\mathcal{T}}(\mathbf{c})\mathbf{s}_{L+M}[n] + \mathbf{v}_M[n] \end{aligned} \tag{3.12}$$

where vec(.) denotes vectorization or stacking of columns of a matrix, and

$$\mathbf{s}_{L+M}[n] = (s[n], s[n-1], \dots, s[n-(L+M)])^T$$

$$\mathbf{v}_M[n] = \mathrm{vec}(\mathbf{v}[n], \mathbf{v}[n-1], \dots, \mathbf{v}[n-M])$$

$$\mathbf{c} = (\mathbf{c}[0], \mathbf{c}[1], \ldots, \mathbf{c}[\mathrm{L}])$$

and $\boldsymbol{\mathcal{T}}(\mathbf{c})$ denotes a block Toeplitz matrix of size (M +1)$n_r$-by-(L + M + 1) with [$\mathbf{c}$, $\mathbf{0}$] as the first $n_r$ rows.

The filter stage consists of three cascaded filters, a N-by-N noise whitening filter (where N is the number of augmented samples by stacking spatially and temporarily adjacent samples), a N-by-1 multi-channel matched filter, and a minimum-phase noise whitening filter. Apparently if we combine the N-by-N noise whitening filter and the N-by-1 multi-channel matched filter together, the combined filter is essentially the same filter as the full-rank space-time equalizer in [33], except that the noise-whitening operation is on the spatio-temporal augmented received sample vector in [11] but on the spatially received sample vector in [33].

Finding the N-by-N noise whitening filter coefficients matrix $\mathbf{W}$ is equivalent to solving the equation $\mathbf{W}^{\mathbf{H}}\mathbf{W}=\boldsymbol{\Lambda}_{\mathrm{M}}^{-1}$, where $\boldsymbol{\Lambda}_{\mathrm{M}} \triangleq \mathrm{E}[\mathrm{v}_{\mathrm{M}}[\mathrm{n}]\mathrm{v}_{\mathrm{M}}[\mathrm{n}]^{\mathrm{H}}]$ is the noise covariance matrix. Accurate estimation of the noise covariance matrix $\boldsymbol{\Lambda}_{\mathrm{M}}$ is nontrivial. Inaccurate estimation may reduce the equalizer performance significantly. [11] implemented two methods to obtain more accurate estimates of the channel, the noise covariance matrix, and the time synchronization position. One method is an iterative approach and the other one finds the channel, the noise covariance matrix, and the time synchronization position directly. We omit details for these two methods as channel estimation is not investigated in this work.

Simulation results in [11] demonstrated that the proposed solution had 0.5-2 dB better BER performance than the VAR-based equalizer [21] and the conventional MLSE equalizer. In the simulation setup, both the desired user and the interferer were GMSK signals. The original channel had four virtual channels by separating the real and imaginary parts and 2x oversampling. Two temporally adjacent sample vectors were stacked hence the final augmented channel matrix contained 8 virtual channels. The VAR-based equalizer had four virtual channels and order-2 VAR model in order to obtain fair comparison. Among the two channel estimated methods in this solution, the computation more intensive iterative parameter estimation method offered about 0.5-1 dB gain w.r.t. the direct channel estimation method.

### 3.1.5 Widely linear rank-1 space-time equalization

In [11] from the previous subsection, one way to create multiple virtual channels is by separating I and Q components of the received complex-valued samples. This real-valued approach is equivalent to widely linear processing (WLP) in [6], in which an invertible unitary transformation matrix can convert a vector in the form of real and imaginary parts into a widely linear form consisting of the vector and its complex conjugate. One straightforward application of WLP in interference cancellation equalization can be found in [13]. The transmission model can be expressed as

$$\mathbf{r}_n = \sum_{k=0}^{L} \mathbf{h}_k d_{n-k} + \sum_{k=0}^{L} \mathbf{c}_k e_{n-k} + \mathbf{n}_{sn} \tag{3.13}$$

where $h_k$ is the k-th tap of the CIR **h** for the desired signal, $c_k$ is the k-th tap of the CIR **c** for the interferer, $d_n$ and $e_n$ are the user's and the interferer's symbols at the symbol interval n, respectively, and $n_{sn}$ denotes the AWGN noise. In that publication, all quantities in the equation are complex-valued scalars as the mobile station has one antenna and symbol spaced sampling is used.

The widely linear and space-time data model creates a 4-by-(Q+1) augmented received sample matrix **R** and a 4-by-(L+1) channel matrix **H** expressed as below

$$R = \begin{bmatrix} \mathbf{r}_k & \mathbf{r}_{k+1} & \cdots & \mathbf{r}_{k+Q} \\ \mathbf{r}_k^* & \mathbf{r}_{k+1}^* & \cdots & \mathbf{r}_{k+Q}^* \\ \mathbf{r}_{k-1} & \mathbf{r}_k & \cdots & \mathbf{r}_{k+Q-1} \\ \mathbf{r}_{k-1}^* & \mathbf{r}_k^* & \cdots & \mathbf{r}_{k+Q-1}^* \end{bmatrix} \quad H = \begin{bmatrix} \mathbf{h}_0 & \cdots & \mathbf{h}_L & \mathbf{0} \\ \mathbf{h}_0^* & \cdots & \mathbf{h}_L^* & \mathbf{0} \\ \mathbf{0} & \mathbf{h}_0 & \cdots & \mathbf{h}_L \\ \mathbf{0} & \mathbf{h}_0^* & \cdots & \mathbf{h}_L^* \end{bmatrix} \tag{3.14}$$

The resulting augmented transmission model can be expressed in a compact matrix form as **R**=**HD**+**CE**+**N**, where **D** is the matrix form of the desired symbols contributing to **R**, **C** is the interference channel matrix with the similar structure as **H**, **E** is the matrix form of the interfering symbols contributing to **R**, and **N** is the matrix form of the additive noise.

The author assumed synchronized network and known training sequence for the interferer. Hence, both **H** and **C** can be estimated first. Then, the optimization is to find the filter coefficient vector maximizing the signal-to-dominant-interference ratio as below

$$\max_{\mathbf{w}} \frac{\|\mathbf{w}^T\mathbf{HD}\|^2}{\|\mathbf{w}^T\mathbf{CE}\|^2} \quad \text{or} \quad \max_{\mathbf{w}} \frac{\mathbf{w}^H(\mathbf{HD})^*(\mathbf{HD})^T\mathbf{w}}{\mathbf{w}^H(\mathbf{CE})^*(\mathbf{CE})^T\mathbf{w}} \tag{3.15}$$

The solution of **w** is a generalized eigenvalue solution

$$\mathbf{w}_{\text{opt}} = \text{eig}\lambda_{\max} \ \ [\text{inv}((\mathbf{CE})^{*}(\mathbf{CE})^{\text{T}})(\mathbf{HD})^{*}(\mathbf{HD})^{\text{T}}] \tag{3.16}$$

And, the overall channel becomes

$$\mathbf{b}_{\text{opt}} = (\mathbf{w}_{\text{opt}}^{\text{T}}\mathbf{H})^{\text{T}} \tag{3.17}$$

Since the noise at the output of the widely linear space-time filter is correlated, a minimum-phase noise whitening filter based on [32] precedes MLSE. Besides whitening the noise, this filter also converts the overall CIR into a minimum phase form, in which the energy is concentrated into the first few taps.

Simulation was performed to verify the single-antenna mobile station performance under TU50 channel profile. Unsurprisingly, this solution was effective when one single interferer existed and $E_b/N_o$ was above 100 dB. However, when $E_b/N_o$ was reduced to 10 dB, the solution performed worse than conventional MAP receiver if C/I was above 5 dB. This is because that the solution only considered the main interferer. Hence, a switch-off algorithm (such as monitoring the C/I) suggested by the author is required to disable the filter when it is undesired. Actually, a more reliable approach without the switch-off algorithm would be maximizing filter output SINR instead of only rejecting the dominant interferer.

## 3.2 Equalizers consisting of complexity-reduction prefilter and JMLSE

The second category of interference cancellation equalizers is multiuser detection or joint detection. One of the most effective algorithms in this category is JMLSE. The standard form of JMLSE is known to be computation intensive, because the number of trellis states (based on all jointly detected users) is exponentially greater than that of a single-user MLSE. Recent years' research has been focusing on the complexity-reduction MIMO prefilter for JMLSE, such as [18, 35] and fast calculation of these filter coefficients [19]. Other design challenges preventing application of JMLSE include accurate channel estimation and correct symbol constellation detection. Specifically, branch metric calculation in JMLSE is sensitive to channel estimation error, especially when the number of trellis states is large; and, sequence detection fails if any of the jointly detected users' symbol constellations is detected incorrectly. Due to reasons above, most practical mobile stations today do not apply multiuser detection at all, or limit the jointly detected users to the desired user plus the strongest interferer only in a synchronized network (in which case interfering base stations are synchronized with the serving base station so that the location of the training sequence of the

interferer is known, which improve the performance of channel estimation and blind symbol constellation detection for the interferer).

In the subsection below, we describe one JMLSE solution adopted in the GSM system. We ignore discussion of the complexity-reduction MIMO prefilters as they are not related to this work.

### 3.2.1 An interference cancellation JMLSE in GSM

Application of the classical vector Viterbi algorithm or JMLSE [16] in GSM was probably first described by [17] and extensive simulation was performed to demonstrate superior BER performance. Since the solution is a relative straightforward application of the classical JMLSE, we only brief the simulation results of some typical GSM test scenarios in that publication.

In the simulation setup, 3 binary sequences, the desired user's signal and two interfering signals, were transmitted over a length-5 TU3 channel (typical urban 3km/h). The receiver used symbol-spaced sampling. To limit the complexity, the desired user and one interferer were jointly detected so that the number of trellis states was 256 ($2^{2*4}$), while the other interferer was not treated specially. The channels for the two jointly detected users were estimated by a conventional least-square method based on the training sequences of the two users, respectively.

For simulation results, under the 3-user but AWGN-free scenario, huge performance gain of about 20 dB by two-user JMLSE was shown, comparing with the conventional MLSE. However, when the power level of the second interferer is strong, such as I1/I2=-5 dB (denoting interference 1 is 5 dB weaker than interferer 2), JMLSE performance approaches the conventional AWGN, according to figure 5 in [16].

## 3.3 Equalizers consisting of (widely) linear filtering and JMLSE

In concept it is straightforward to extend the first category of interference cancellation equalizers, which consists of an interference cancellation filter and single-user MLSE, into this category of filter plus JMLSE solutions. Besides using JMLSE to jointly detect multiple users, design in the filter stage lies in the categorization of wanted signals vs. disturbance. Typically the desired user and a few interferers can be deemed as wanted signals, and the rest interferers and background noise are considered as disturbance. In the selection of those interferers belonging to wanted signals, they may satisfy several criteria such as strong signal strength, burst-wise synchronized with the desired user, having low-order modulation (GMSK instead of 8PSK). Once wanted signals and disturbance are

divided, the optimization algorithms of the MMSE, maximum SINR, or noise whitening filters in the first category of equalizers can be modified straightforwardly to suppress disturbance but pass wanted signals to JMLSE.

In the following subsection, we present one recent solution proposed for VAMOS mobile station equalization.

### 3.3.1 Single Antenna MIMO (SAM) receiver for VAMOS

The idea we discussed above has been utilized in [20] to propose a VAMOS mobile station equalizer dubbed single antenna MIMO (SAM) receiver. In that proposal, the two paired VAMOS users belong to wanted signals. This is a practical approach because the paired VAMOS user meets our selection criteria of wanted signals for JMLSE. In particular, it is relatively strong, exactly synchronized with the desired user, propagates through the same radio channel, and binary modulated. In that proposal, the overall channel is deemed as a 2-input (denoting the two paired VAMOS users transmitting binary symbol sequences) and 2-output (denoting the real and imaginary parts of the received temporal samples from the single mobile station antenna) real-valued channel matrix; and, the interference plus noise is modeled as a vector valued auto-regressive (VAR) process based on [21]. Hence, the equalizer is a straightforward extension of the spatio-temporal interference rejection algorithm in [21], which we have discussed in subsection 3.1.3. To be specific, in the first stage, with a VAR model to approximate interference plus noise, a finite impulse response (FIR) filter with the same order is able to whiten the spatially and temporally correlated interference plus noise. In the second stage, a conventional two-user JMLSE detects the two VAMOS binary symbol sequences jointly.

Other than information above, detailed design was not discussed in [20], because the authors indicated that the intention was to provide a proof of concept. Extensive simulation in that report confirmed that this proposed JMLSE equalizer obtained better frame error rate (FER) performance than the comparing legacy SAIC single-MLSE equalizer. Both equalizers used the same VAR-modeling based noise whitening filter.

# Chapter 4
# The proposed VAMOS equalizer

As having mentioned in the introduction chapter, this work proposes a two-stage equalizer for single-antenna mobile stations operating in VAMOS mode. It consists of a reduced-rank widely linear MIMO MMSE filter and a JMLSE. Some trivial modification to the conventional JMLSE is proposed, but novelty mainly lies in various techniques in the filter design, as explained below.

Widely linear processing is a suitable technique to improve filter output SINR in VAMOS operating mode, because the transmitted VAMOS signal may be improper due to α-QPSK modulation or the interfering signals may be improper due to some modulation types.

The filter structure takes a MIMO form, corresponding to multiple-virtual-channel CIR approach introduced in section 3.1. The multiple-virtual-channel CIR matrix has N rows and M columns, where N denotes the number of augmented samples at the channel output during each symbol period and M denotes the temporal length of CIR.

Reduced-rank processing is an effective method to achieve computation efficiency and robustness against disturbance and model mismatch, usually via singular value decomposition (SVD) [36]. This technique is desired for VAMOS equalizer design where computation reduction is desired and strong CCI degrades channel estimation. In the proposed equalizer, we assume a low rank model of the augmented channel matrix with rank r <min(N, M). As a result, the MIMO filter has N inputs (due to N augmented samples per symbol period) and r outputs (due to r principal components in the rank-r channel matrix assumption [6] ).

A constrained MMSE algorithm instead of a noise whitening algorithm is used to improve filter performance because in most practical situations estimates of second order statistics used to calculate filter coefficients are inaccurate. As the post-filter TIR and filter coefficients are jointly optimized in the MMSE algorithm, constraints are required to avoid trivial solutions (such as zero-valued TIR and filter coefficients which yield zero MSE but completely suppress the wanted signals). The orthonormality constraint (ONC) in [37] is found in this chapter to be optimum in the sense that it enables the overall equalizer equivalent to the noise whitening filter based MLSE [33]. It is known in [22] that noise whitening filter transforms a system disturbed by the correlated Gaussian noise into one disturbed by white Gaussian noise without loss of information, and MLSE is the optimum solution in the white Gaussian noise situation. Note that to achieve full equivalence to the optimum

noise whitening filter based MLSE, a TIR correction and noise balance unit needs to be placed between the MMSE filter and JMLSE, as we will describe momentarily.

This chapter contains two sections. The first section gives detailed description of the equalizer design, and the second section proves the equivalence between the proposed equalizer and the optimum noise whitening filter based MLSE.

## 4.1 Detailed description of the proposed VAMOS equalizer

The VAMOS transmission model diagram from chapter 2 is repeated here with some modification. Unlike in chapter 2 where we intends to differentiate various parts in the transmitter and the receiver, in this chapter the channel matrix **H** covers rotation and LGMSK pulse shaping at the transmitter and the channel selection filter and derotation at the receiver, in order to obtain an overall discrete-time CIR from the equalizer's perspective.

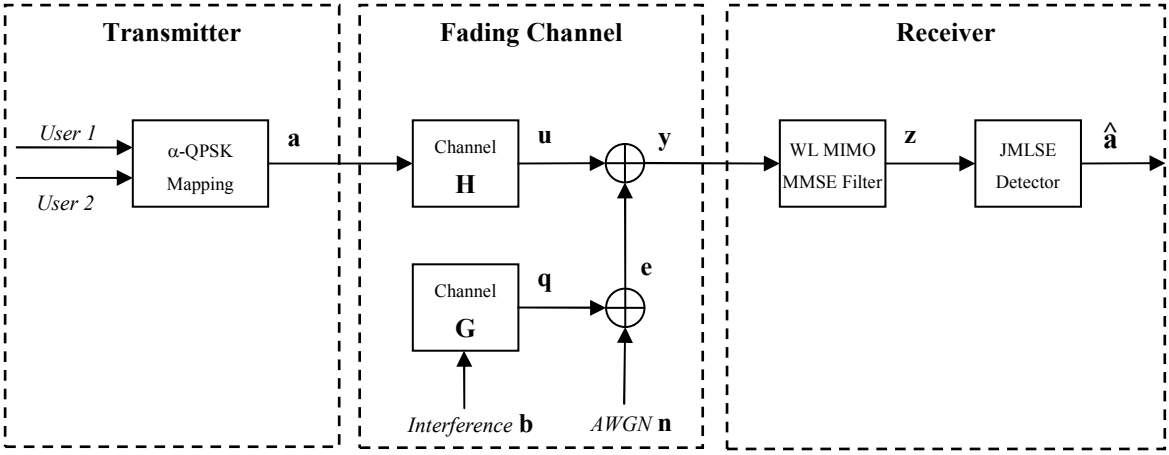


**Figure 4.1 The discrete-time baseband transmission model**

With 2x oversampling, the received sample vector at interval k can be expressed as

$$\mathbf{y}(k) = \sum_{l=0}^{L-1} \mathbf{h}(l)a(k-l) + \sum_{i=0}^{I-1}\sum_{j=0}^{L-1} \mathbf{g}_i(j)b_i(k-j) + \mathbf{n}(k) = \mathbf{H}\mathbf{a}_L(k) + \mathbf{e}(k) \qquad (4.1)$$

Here, L is the overall CIR length, **H** is the 2-by-L channel matrix, $\mathbf{a}_L(k)$ is the transmitted symbol vector consisting of the current and previous L-1 transmitted symbols (each of these symbols is a complex value whose real and imaginary parts are from the two paired VAMOS users respectively), **e**(k) is the 2-by-1 disturbance vector contributed by interference and noise.

### 4.1.1 The derivation of the real-valued form of the widely linear MIMO MMSE filter

Assuming 2x oversampling and N is a multiple of 2 (which is not necessary but simplify the notation), by stacking (N/2) temporally adjacent received sample vectors **y**(k), …, **y**(k-N/2+1), the MIMO filtering operation can be expressed as

$$\mathbf{z}(\mathrm{k}) = \mathbf{F}_{\mathrm{N}}^{\mathrm{H}}\mathbf{y}_{\mathrm{N}}(\mathrm{k}) = \mathbf{F}_{\mathrm{N}}^{\mathrm{H}}\underline{\mathbf{H}}\mathbf{a}_{\mathrm{L+N/2-1}}(\mathrm{k}) + \mathbf{F}_{\mathrm{N}}^{\mathrm{H}}\mathbf{e}_{\mathrm{N}}(\mathrm{k}) \tag{4.2}$$

where **z**(k) is the length-r filter output vector at interval k,

the N-by-r filter coefficient matrix is defined as

$$\mathbf{F}_{\mathrm{N}} \triangleq \begin{bmatrix} \mathrm{f}_{1,1} \ldots \mathrm{f}_{1,\mathrm{r}} \\ \mathrm{f}_{2,1} \ldots \mathrm{f}_{2,\mathrm{r}} \\ \vdots \\ \mathrm{f}_{\mathrm{N},1} \ldots \mathrm{f}_{\mathrm{N},\mathrm{r}} \end{bmatrix}$$

the N-by-(L+N/2-1) channel matrix is defined as

$$\underline{\mathbf{H}} = \begin{bmatrix} \mathrm{h}(0) & \ldots & \mathrm{h}(\mathrm{L}-1) & 0 & \ldots & 0 \\ & \mathrm{h}(0) & \ldots & \mathrm{h}(\mathrm{L}-1) & 0 & \ldots \\ & & \ldots & \ldots & \ldots & 0 \\ & & & \mathrm{h}(0) & \ldots & \mathrm{h}(\mathrm{L}-1) \end{bmatrix}$$

the length-N augmented received sample vector is defined as

$$\mathbf{y}_{\mathrm{N}}(\mathrm{k}) \triangleq \begin{bmatrix} \mathrm{y}(\mathrm{k}) \\ \mathrm{y}(\mathrm{k}-1) \\ \vdots \\ \mathrm{y}(\mathrm{k}-\mathrm{N}/2+1) \end{bmatrix}$$

the length-(L+N/2-1) transmitted symbol vector is defined as

$$\mathbf{a}_{\mathrm{L+N/2-1}}(\mathrm{k}) \triangleq \begin{bmatrix} \mathrm{a}(\mathrm{k}) \\ \mathrm{a}(\mathrm{k}-1) \\ \vdots \\ \mathrm{a}(\mathrm{k}-\mathrm{L}-\mathrm{N}/2+2) \end{bmatrix}$$

the length-N augmented disturbance vector is

$$\mathbf{e}_{\mathrm{N}}(\mathrm{k}) \triangleq \begin{bmatrix} \mathrm{e}(\mathrm{k}) \\ \mathrm{e}(\mathrm{k}-1) \\ \vdots \\ \mathrm{e}(\mathrm{k}-\mathrm{N}/2+1) \end{bmatrix}$$

From now on we define M= L+N/2-1 to simplify notation. Hence, the augmented channel matrix $\underline{H}$ is N-by-M.

At interval k, since the augmented received sample vector $\mathbf{y}_N(k)$ and the transmitted symbol vector $\mathbf{a}_{L+N/2-1}(k)$ may be jointly improper, we can apply WLP to filter the augmented $\mathbf{y}_N(k)$ and its conjugate version

$$\mathbf{z}_{WL}(k) = \mathbf{F}_{WL}^{H}\begin{bmatrix}\mathbf{y}_N(k)\\ \mathbf{y}_N(k)^*\end{bmatrix} = \mathbf{F}_{WL}^{H}\underline{\mathbf{H}}_{WL}\begin{bmatrix}\mathbf{a}_M(k)\\ \mathbf{a}_M(k)^*\end{bmatrix} + \mathbf{F}_{WL}^{H}\begin{bmatrix}\mathbf{e}_N(k)\\ \mathbf{e}_N(k)^*\end{bmatrix} \tag{4.3}$$

where we have replaced $\mathbf{a}_{L+N/2-1}(k)$ with $\mathbf{a}_M(k)$ to simplify the expression.

Now at the filter output, the overall channel matrix becomes $\mathbf{F}_{WL}^{H}\underline{\mathbf{H}}_{WL}$. If a conventional vector-input Forney-type JMLSE is used to detect the transmitted symbol sequences of the two paired VAMOS users, the trellis states should be expressed as $s_k \triangleq \{a(k-1), \dots, a(k-M+1), a^*(k-1), \dots, a^*(k-M+1)\}$. Due to the equivalence between the widely linear complex-valued filter and the linear real-valued filter [6] and also the equivalent trellis state expression between $s_k \triangleq \{a(k-1), \dots, a(k-M+1), a^*(k-1), \dots, a^*(k-M+1)\}$ and $s_{k,real} \triangleq \{Re[a(k-1)], Im[a(k-1)], \dots, Re[a(k-M+1)], Im[a(k-M+1)]\}$, we convert the widely linear filter into a real-valued form

$$\mathbf{z}_{real}(k) = \mathbf{F}_{real}^{H}\mathbf{y}_{N,real}(k) = \mathbf{F}_{real}^{H}\cdot\underline{\mathbf{H}}_{real}\cdot\mathbf{a}_{M,real}(k) + \mathbf{F}_{real}^{H}\cdot\mathbf{e}_{N,real}(k) \tag{4.4}$$

where

$$\underline{\mathbf{H}}_{real} = \begin{bmatrix}Re\{\underline{\mathbf{H}}\} & -Im\{\underline{\mathbf{H}}\}\\ Im\{\underline{\mathbf{H}}\} & Re\{\underline{\mathbf{H}}\}\end{bmatrix}$$

$$\mathbf{y}_{N,real}(k) = \begin{bmatrix}Re\{\mathbf{y}_N(k)\}\\ Im\{\mathbf{y}_N(k)\}\end{bmatrix}$$

$$\mathbf{a}_{M,real}(k) = \begin{bmatrix}Re\{\mathbf{a}_M(k)\}\\ Im\{\mathbf{a}_M(k)\}\end{bmatrix}$$

$$\mathbf{e}_{N,real}(k) = \begin{bmatrix}Re\{\mathbf{e}_N(k)\}\\ Im\{\mathbf{e}_N(k)\}\end{bmatrix}$$

After the MIMO filter structure is defined, the optimization algorithm calculating the coefficient matrix $\mathbf{F}_{real}$ needs to be decided. In general, there are three types of optimization algorithms, maximum SINR, noise whitening, and MMSE, respectively. The first two algorithms require known

or estimated autocovariance matrix of the disturbance. Maximum SINR algorithm attempts to maximize the energy of the wanted signals w.r.t. the energy of the disturbance; noise whitening filter attempts to whiten the disturbance. As we have discussed, in general it is difficult to estimate second order statistics of the disturbance because training sequence of it is unknown. Therefore, MMSE is a more robust approach in this case. Computation of MMSE filter coefficient matrix is based on CIR of the wanted signals and the autocovariance matrix of the received signals (whose samples are directly available). Most of recent years' MMSE algorithms jointly optimize the filter coefficient matrix and the post-filter TIR to minimize the filter output MSE. Constraining the TIR matrix avoids trivial solutions such as both filter coefficient matrix and the post-filter TIR are zero. The MMSE filter in our work is based on the feed forward filter part of the MMSE-DFE in [37]. Application of this filter in widely linear processing was shown in [38], where the authors suggested a widely linear MMSE-DFE equalizer with the identity tap constraint (ITC) (which constrains the first matrix tap of TIR to be an identity matrix, as defined in [37]). In our proposed widely linear MMSE filter, the orthonormality constraint (ONC) defined in [37] is selected, which constrain the Hermitian transpose of the TIR matrix to consist of r orthonormal columns (or equivalently the TIR matrix to consist of r orthonormal rows). With this ONC-based MMSE algorithm, the residue disturbance components among the r different filter outputs are uncorrelated but have unequal powers. Therefore, a simple noise balance unit follows the ONC-based MMSE filter to ensure equal power and uncorrelation of the residue disturbance among different filter outputs. In the next section, we will prove that the cascade of the ONC-constraint MMSE filter, noise balance filter, and JMLSE offers optimum equalization in the sense that it enables the overall equalizer equivalent to the optimum noise whitening filter based MLSE [33].

Now we derive the ONC-based MMSE algorithm in the real-valued filter structure. The filter coefficient matrix $\mathbf{F}_{\text{real}}$ has been defined above. If we denote the TIR channel matrix as $\mathbf{B}^{\text{H}}$, the filter output MSE is

$$\text{trace}(\mathbf{R}_{\text{ee}}) \triangleq \text{trace}\left(\text{E}[\mathbf{e}(\text{k})\mathbf{e}(\text{k})^{\text{H}}]\right)$$

$$= \text{trace}\left(\text{E}\left[\left(\mathbf{F}_{\text{real}}^{\text{H}}\mathbf{y}_{\text{N,real}}(\text{k}) - \mathbf{B}^{\text{H}}\mathbf{a}_{\text{M,real}}(\text{k})\right)\left(\mathbf{F}_{\text{real}}^{\text{H}}\mathbf{y}_{\text{N,real}}(\text{k}) - \mathbf{B}^{\text{H}}\mathbf{a}_{\text{M,real}}(\text{k})\right)^{\text{H}}\right]\right) \quad (4.5)$$

[37] assumed that the non-linear detector is the feedback filter of the MIMO MMSE DFE; hence, the number of outputs of the feedforward filter is equal to the number of jointly detected users. In our

case, the number of output r of $\mathbf{F}_{\mathrm{real}}^{\mathrm{H}}$ can be any value because the following detector is a vector-input Forney-type JMLSE.

Due to the Orthogonality Principle which states that $\mathrm{E}\left[\mathbf{e}_{\mathrm{N,real}}(\mathrm{k})\mathbf{y}^{\mathrm{H}}{}_{\mathrm{N,real}}(\mathrm{k})\right] = \mathbf{0}$ [37] (note that we have replaced $\mathbf{E}_{\mathrm{k}}$ and $\mathbf{y}^{*}{}_{\mathrm{k+Nf-1:k}}$ in [37] with our notations), we have the relation that $\mathbf{F}_{\mathrm{real}}^{\mathrm{H}}\mathbf{R}_{\mathrm{yy}} = \mathbf{B}^{\mathrm{H}}\mathbf{R}_{\mathrm{ay}}$, or equivalently $\mathbf{F}_{\mathrm{real}}^{\mathrm{H}} = \mathbf{B}^{\mathrm{H}}\mathbf{R}_{\mathrm{ay}}\mathbf{R}_{\mathrm{yy}}^{-1}$ and $\mathbf{F}_{\mathrm{real}} = \mathbf{R}_{\mathrm{yy}}^{-1}\mathbf{R}_{\mathrm{ya}}\mathbf{B}$. Hence, joint optimization of $\mathbf{F}_{\mathrm{real}}$ and $\mathbf{B}$ can be derived by substituting $\mathbf{F}_{\mathrm{real}}$ with $\mathbf{R}_{\mathrm{yy}}^{-1}\mathbf{R}_{\mathrm{ya}}\mathbf{B}$ into the MMSE cost function as below [37]

$$\mathrm{trace}(\mathbf{R}_{\mathrm{ee}}) \triangleq \mathrm{trace}(\mathrm{E}[\mathbf{e}(\mathrm{k})\mathbf{e}(\mathrm{k})^{\mathrm{H}}])$$

$$= \mathrm{trace}\left(\mathrm{E}\left[\left(\mathbf{F}_{\mathrm{real}}^{\mathrm{H}}\mathbf{y}_{\mathrm{N,real}}(\mathrm{k}) - \mathbf{B}^{\mathrm{H}}\mathbf{a}_{\mathrm{M,real}}(\mathrm{k})\right)\left(\mathbf{F}_{\mathrm{real}}^{\mathrm{H}}\mathbf{y}_{\mathrm{N,real}}(\mathrm{k}) - \mathbf{B}^{\mathrm{H}}\mathbf{a}_{\mathrm{M,real}}(\mathrm{k})\right)^{\mathrm{H}}\right]\right)$$

$$= \mathrm{trace}\left(\mathbf{B}^{\mathrm{H}}\left(\mathbf{R}_{\mathrm{aa}} - \mathbf{R}_{\mathrm{ay}}\mathbf{R}_{\mathrm{yy}}^{-1}\mathbf{R}_{\mathrm{ya}}\right)\mathbf{B}\right) \tag{4.6}$$

Under the ONC constraint that $\mathbf{B}$ has orthonormal columns or equivalently $\mathbf{B}^{\mathrm{H}}$ has orthonormal rows, [37] found that the optimum $\mathbf{B}$, denoted by $\mathbf{B}_{\mathrm{opt}}$, consists of r eigenvectors corresponding to the r smallest eigenvalues of $\mathbf{R}_{\mathrm{aa}} - \mathbf{R}_{\mathrm{ay}}\mathbf{R}_{\mathrm{yy}}^{-1}\mathbf{R}_{\mathrm{ya}}$ (we have used r, instead $\mathrm{n_i}$ denoting the number of jointly detected users in [37], to emphasize that the number of MMSE filter outputs in our solution is scalable instead of having to be equal to the number of users).

After finding $\mathbf{B}_{\mathrm{opt}}$, it is straightforward to calculate the optimum MMSE filter coefficients matrix $\mathbf{F}_{\mathrm{opt}} = \mathbf{R}_{\mathrm{yy}}^{-1}\mathbf{R}_{\mathrm{ya}}\mathbf{B}_{\mathrm{opt}}$. With $\mathbf{B}_{\mathrm{opt}}$ consisting of r eigenvectors of $\mathbf{R}_{\mathrm{aa}} - \mathbf{R}_{\mathrm{ay}}\mathbf{R}_{\mathrm{yy}}^{-1}\mathbf{R}_{\mathrm{ya}}$, the filter output noise autocovariance matrix $\mathbf{R}_{\mathrm{ee,min}}$ is obviously diagonal, with each diagonal entry representing the power of the residue disturbance at each filter output tap, respectively.

### 4.1.2 The TIR correction and noise balance unit

In order to optimize the equalizer, two adjustments, TIR correction and noise balance, need to be provided between the MMSE filter and the JMLSE.

Regarding TIR correction, it is known that in general the MMSE filter output is biased and removing the bias improves the BER performance [39]. In our case, the actual post-filter CIR $\mathbf{B}_{\mathrm{actual}}^{\mathrm{H}} = \mathbf{F}_{\mathrm{opt}}^{\mathrm{H}}\underline{\mathbf{H}}_{\mathrm{real}}$ is not equal to the TIR matrix $\mathbf{B}_{\mathrm{opt}}^{\mathrm{H}}$ obtained in the MMSE filter optimization. In section 4.2, we will find that $\mathbf{B}_{\mathrm{actual}}^{\mathrm{H}} = \mathbf{F}_{\mathrm{opt}}^{\mathrm{H}}\underline{\mathbf{H}}_{\mathrm{real}} = \left(\mathbf{I} - \mathbf{R}_{\mathrm{ee,min}}\right)\mathbf{B}_{\mathrm{opt}}^{\mathrm{H}}$. Since $\mathbf{B}_{\mathrm{opt}}$ consists of r eigenvectors of $\mathbf{R}_{\mathrm{aa}} - \mathbf{R}_{\mathrm{ay}}\mathbf{R}_{\mathrm{yy}}^{-1}\mathbf{R}_{\mathrm{ya}}$ and $\mathbf{B}_{\mathrm{actual}}$ consists of scaled column vectors of $\mathbf{B}_{\mathrm{opt}}$, the

resulting unbiased noise autocovariance matrix $\mathbf{R}_{\mathrm{ee,actual}} = \mathbf{B}^{\mathrm{H}}_{\mathrm{actual}}(\mathbf{R}_{\mathrm{aa}} - \mathbf{R}_{\mathrm{ay}}\mathbf{R}^{-1}_{\mathrm{yy}}\mathbf{R}_{\mathrm{ya}})\mathbf{B}_{\mathrm{actual}}$ is still a diagonal matrix, with each diagonal entry representing the power of the residue disturbance at each filter output tap, respectively.

JMLSE expects spatially white noise at its input. We have shown that $\mathbf{R}_{\mathrm{ee,actual}}$ is a diagonal matrix, revealing that the unbiased residue disturbance among r filter outputs is uncorrelated. Hence, whitening the residue disturbance, or finding $\mathbf{R}^{-1/2}_{\mathrm{ee,actual}}$, is a computation trivial task. Since in the simulation r=2 is chosen, we simply keep the first filter output intact and scale the second filter output by $\sqrt{\mathbf{R}_{\mathrm{ee,actual}}(1,1)/\mathbf{R}_{\mathrm{ee,actual}}(2,2)}$.

Note that the actual "post noise balance unit" CIR is $\mathbf{B}^{\mathrm{H}}_{\mathrm{overall}} = \mathbf{R}^{-1/2}_{\mathrm{ee,actual}}\mathbf{F}^{\mathrm{H}}_{\mathrm{opt}}\underline{\mathbf{H}}_{\mathrm{real}}$. This is the overall CIR for the following JMLSE.

### 4.1.3 The two-user JMLSE

In the proposed solution, we use a standard JMLSE with trivial modification. Some adjustments are described as below, in order to use the existing joint MLSE equalizer directly.

For a standard JMLSE, we know that for CIRs spanning M symbol periods, the trellis state at interval k is defined as

$$\mathrm{s}_{\mathrm{k,real}} \triangleq \{\mathrm{Re}[\mathrm{a}(\mathrm{k}-1)], \mathrm{Im}[\mathrm{a}(\mathrm{k}-1)], \ldots, \mathrm{Re}[\mathrm{a}(\mathrm{k}-\mathrm{M}+1)], \mathrm{Im}[\mathrm{a}(\mathrm{k}-\mathrm{M}+1)]\} \qquad (4.7)$$

In the previous augmented space-time data model, the transmitted symbol sequence was

$$\mathbf{a}_{\mathrm{M,real}}(\mathrm{k}) = \begin{bmatrix} \mathrm{Re}\{\mathbf{a}_{\mathrm{M}}(\mathrm{k})\} \\ \mathrm{Im}\{\mathbf{a}_{\mathrm{M}}(\mathrm{k})\} \end{bmatrix} \qquad (4.8)$$

Hence, the post-filter TIR matrix $\mathbf{B}^{\mathrm{H}}_{\mathrm{overall}}$ corresponds to the sequence of {Re{a(k)}, …, Re{a(k-M+1)}, Im{a(k)}, …, Im{a(k-M+1)}}, instead of the trellis state defined above. This is trivial and we just need to reorder entries in $\mathbf{B}^{\mathrm{H}}_{\mathrm{overall}}$ after the filter stage; or more efficiently as done in our actual implementation, we re-arrange the augmented real-valued received sample vector $\mathbf{y}_{\mathrm{N,real}}(\mathrm{k})$ and the augmented channel matrix $\underline{\mathbf{H}}_{\mathrm{real}}$ correspondingly in the MMSE filtering stage. The only reason we expressed $\mathbf{y}_{\mathrm{N,real}}(\mathrm{k})$ in the form of $[\mathrm{Re}\{\mathbf{y}_{\mathrm{N}}(\mathrm{k})\}^{\mathrm{T}} \;\; \mathrm{Im}\{\mathbf{y}_{\mathrm{N}}(\mathrm{k})\}^{\mathrm{T}}]^{\mathrm{T}}$ previously was to have a compact expression and also follow the customary expression in most WLP publications.

## 4.2 Theoretical analysis of the equalizer

In this section we prove a proposition that the proposed equalizer is equivalent to the optimum noise whitening filter based MLSE. The proposition is applicable to full rank and reduced rank channel models. In the proof we will find that the number of outputs of the MMSE filter is equal to the rank of the channel matrix. The proposition applies to widely linear and linear filter, and single-user MLSE and joint MLSE.

Proposition: The cascade of the N-input r-output ONC-based MMSE filter, the TIR correction and noise balance unit, and MLSE is equivalent to the N-input noise whitening filter based MLSE with the rank r channel matrix.

Proof: Let us study the standard noise whitening filter based MLSE equalizer first. We define the rank r channel matrix after noise whitening filter $\mathbf{R}_{nn}^{-1/2}$ as $\mathbf{H}_{NW} \triangleq \mathbf{R}_{nn}^{-1/2}\mathbf{H}$, which is a N-by-M matrix with rank r≤min(N, M). Perform SVD to factorize $\mathbf{H}_{NW}$ as $\mathbf{H}_{NW} = \mathbf{U}_r\mathbf{D}_r\mathbf{V}_r^H$, where $\mathbf{U}_r$ is a N-by-r unitary matrix, $\mathbf{V}_r$ is a M-by-r unitary matrix, and $\mathbf{D}_r$ is a r-by-r diagonal matrix. This is a compact form of SVD by considering the fact that the diagonal matrix $\mathbf{D}$ in the standard form of SVD contains only r positive singular values along its diagonal. At symbol interval k, if we denote the length-N received sample vector as $\mathbf{y}_N(k)$ and the length-N noise-whitened vector as $\mathbf{z}_N(k) = \mathbf{R}_{nn}^{-1/2}\mathbf{y}_N(k)$, the k-th Euclidean-distance branch metric of the standard MLSE is as below, where $\mathbf{a}_M(k)$ denotes the length-M transmitted symbol vector consisting of the current and the previous M-1 transmitted symbols.

$$
\begin{aligned}
L\{\mathbf{a}_M(k)\} &= \|\mathbf{z}_N(k) - \mathbf{H}_{NW}\mathbf{a}_M(k)\|^2 \\
&= \left(\mathbf{z}_N^H(k) - \mathbf{a}_M^H(k)\mathbf{H}_{NW}^H\right)\left(\mathbf{z}_N(k) - \mathbf{H}_{NW}\mathbf{a}_M(k)\right) \\
&= \mathbf{z}_N^H(k)\mathbf{z}_N(k) - \mathbf{z}_N^H(k)\mathbf{H}_{NW}\mathbf{a}_M(k) - \mathbf{a}_M^H(k)\mathbf{H}_{NW}^H\mathbf{z}_N(k) + \mathbf{a}_M^H(k)\mathbf{H}_{NW}^H\mathbf{H}_{NW}\mathbf{a}_M(k) \\
&= \mathbf{z}_N^H(k)\mathbf{z}_N(k) - \mathbf{z}_N^H(k)\mathbf{H}_{NW}\mathbf{a}_M(k) - \mathbf{a}_M^H(k)\mathbf{H}_{NW}^H\mathbf{z}_N(k) + \mathbf{a}_M^H(k)\mathbf{V}_r\mathbf{D}_r\mathbf{U}_r^H\mathbf{U}_r\mathbf{D}_rV_r^H\mathbf{a}_M(k) \\
&= C - \mathbf{z}_N^H(k)\mathbf{U}_r\mathbf{D}_r\mathbf{V}_r^H\mathbf{a}_M(k) - \mathbf{a}_M^H(k)\mathbf{V}_r\mathbf{D}_r\mathbf{U}_r^H\mathbf{z}_N(k) + \mathbf{a}_M^H(k)\mathbf{V}_r\mathbf{D}_r^2\mathbf{V}_r^H\mathbf{a}_M(k) \qquad (4.9)
\end{aligned}
$$

In the equations above, we use C to denote $\mathbf{z}_N^H(k)\mathbf{z}_N(k)$, a quantity independent of $\mathbf{a}_M(k)$. Therefore, the selection of a MLSE output sequence among all possible sequences depends on terms other than C in (4.9). In other words, replacing C by any value $C_1$ independent of $\mathbf{a}_M(k)$ in branch

metric calculation in (4.9) does not change the MLSE output sequence. If we define $C_1 = \mathbf{z}_N^H(k)\mathbf{U}_r\mathbf{U}_r^H\mathbf{z}_N(k)$, the new branch metric becomes

$$L_1\{\mathbf{a}_M(k)\} = C_1 - \mathbf{z}_N^H(k)\mathbf{U}_r\mathbf{D}_r\mathbf{V}_r^H\mathbf{a}_M(k) - \mathbf{a}_M^H(k)\mathbf{V}_r\mathbf{D}_r\mathbf{U}_r^H\mathbf{z}_N(k) + \mathbf{a}_M^H(k)\mathbf{V}_r\mathbf{D}_r^2\mathbf{V}_r^H\mathbf{a}_M(k)$$

$$= \mathbf{z}_N^H(k)\mathbf{U}_r\mathbf{U}_r^H\mathbf{z}_N(k) - z_N^H(k)\mathbf{U}_r\mathbf{D}_r\mathbf{V}_r^H a_M(k) - \mathbf{a}_M^H(k)\mathbf{V}_r\mathbf{D}_r\mathbf{U}_r^H\mathbf{z}_N(k) + \mathbf{a}_M^H(k)\mathbf{V}_r\mathbf{D}_r^2\mathbf{V}_r^H\mathbf{a}_M(k)$$

$$= \left(\mathbf{z}_N^H(k)\mathbf{U}_r - \mathbf{a}_M^H(k)\mathbf{V}_r\mathbf{D}_r\right)\left(\mathbf{U}_r^H\mathbf{z}_N(k) - \mathbf{D}_r\mathbf{V}_r^H\mathbf{a}_M(k)\right)$$

$$= \left\|\mathbf{U}_r^H\mathbf{z}_N(k) - \mathbf{D}_r\mathbf{V}_r^H\mathbf{a}_M(k)\right\|^2$$

$$= \left\|\mathbf{U}_r^H\mathbf{R}_{nn}^{-1/2}\mathbf{y}_N(k) - \mathbf{D}_r\mathbf{V}_r^H\mathbf{a}_M(k)\right\|^2 \qquad (4.10)$$

In the last line above, we can consider $\mathbf{U}_r^H\mathbf{R}_{nn}^{-1/2}$ as a matrix filter processing the length-N received sample vector and producing a length-r output vector, and $\mathbf{D}_r\mathbf{V}_r^H$ as the r-by-M post-filter overall channel matrix. This new expression (4.10) is dubbed as modified noise whitening filter based MLSE. The two MLSE equalizers are equivalent because they output the same detected sequence. A diagram of the two equalizers is shown below.

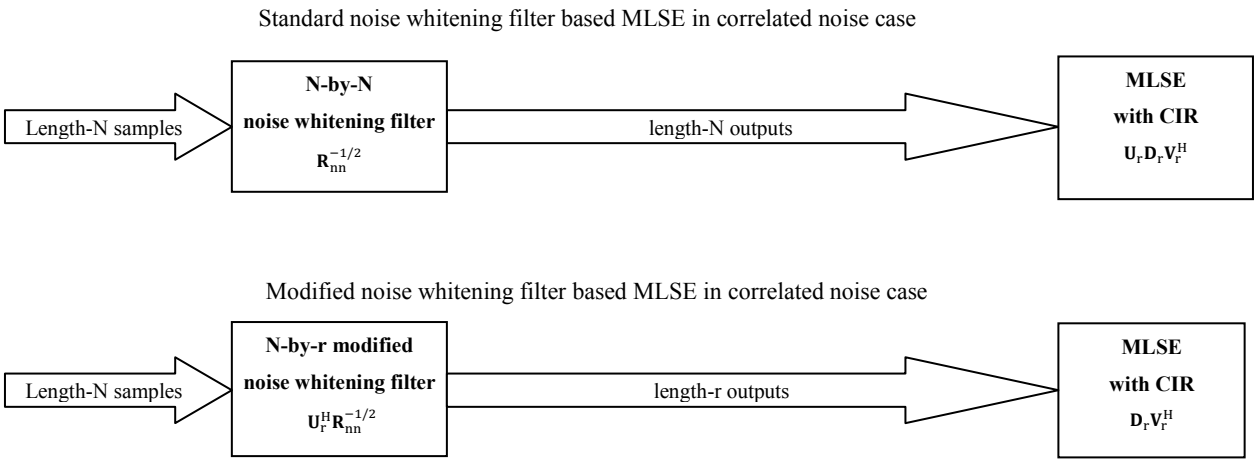


**Figure 4.2 Two equivalent noise whitening filter based MLSE equalizers with the rank r channel model**

Next, let us find the equivalence between the modified noise whitening filter based MLSE and our proposed MMSE filter based equalizer.

In subsection 4.1.1, we have shown that due to the ONC constraint, $\mathbf{B}$ consists of r eigenvectors corresponding to the r smallest eigenvalues of $\mathbf{R}_{aa} - \mathbf{R}_{ay}\mathbf{R}_{yy}^{-1}\mathbf{R}_{ya}$, where the subscript *y* denotes the augmented received sample vector and the subscript *a* denotes the transmitted symbol vector. We then have the following series of derivation based on [40].

$$\mathbf{R}_{ee} \triangleq \mathrm{E}[\mathbf{e}(\mathrm{k})\mathbf{e}(\mathrm{k})^{\mathrm{H}}]$$

$$= \mathbf{B}^{\mathrm{H}}\left(\mathbf{R}_{aa} - \mathbf{R}_{ay}\mathbf{R}_{yy}^{-1}\mathbf{R}_{ya}\right)\mathbf{B}$$

$$= \mathbf{B}^{\mathrm{H}}\left(\mathbf{R}_{aa} - \mathbf{R}_{aa}\mathrm{H}^{\mathrm{H}}(\mathbf{H}\mathbf{R}_{aa}\mathrm{H}^{\mathrm{H}} + \mathbf{R}_{nn})^{-1}\mathbf{H}\mathbf{R}_{aa}\right)\mathbf{B}$$

$$= \mathbf{B}^{\mathrm{H}}\left(\mathbf{R}_{aa}^{-1} + \mathbf{H}^{\mathrm{H}}\mathbf{R}_{nn}^{-1}\mathbf{H}\right)^{-1}\mathrm{B}$$

$$= \mathbf{B}^{\mathrm{H}}\left(\mathbf{R}_{aa}^{-1} + \mathbf{H}^{\mathrm{H}}\mathbf{R}_{nn}^{-\mathrm{H}/2}\mathbf{R}_{nn}^{-1/2}\mathbf{H}\right)^{-1}\mathbf{B}$$

$$= \mathbf{B}^{\mathrm{H}}\left(\mathbf{R}_{aa}^{-1} + (\mathbf{R}_{nn}^{-1/2}\mathbf{H})^{\mathrm{H}}\mathbf{R}_{nn}^{-1/2}\mathbf{H}\right)^{-1}\mathbf{B}$$

$$= \mathbf{B}^{\mathrm{H}}\left(\mathbf{I} + (\mathbf{R}_{nn}^{-1/2}\mathbf{H})^{\mathrm{H}}\mathbf{R}_{nn}^{-1/2}\mathbf{H}\right)^{-1}\mathbf{B} \tag{4.11}$$

The last line is due to the fact that the transmitted symbol sequence is i.i.d. in VAMOS (which is also true in many other communication systems); hence, the autocorrelation matrix of the transmitted symbol vector is an identity matrix. Since $\mathbf{R}_{nn}^{-1/2}\mathbf{H}$ is the post noise-whitening-filter channel matrix $\mathbf{H}_{NW}$, it can be factorized by SVD as $\mathbf{H}_{NW} = \mathbf{U}_M\mathbf{D}_M\mathbf{V}_M^H$, where $\mathbf{U}_M$ is a N-by-M unitary matrix, $\mathbf{V}_M$ is a M-by-M unitary matrix, and $\mathbf{D}_M$ is a M-by-M diagonal matrix consisting of M singular values, in which the first r values are positive and arranged in descending order and the other M-r values are zero. We then have

$$\mathbf{R}_{ee} = \mathbf{B}^{\mathrm{H}}\left(\mathbf{I} + \mathbf{H}_{NW}^{\mathrm{H}}\mathbf{H}_{NW}\right)^{-1}\mathbf{B}$$

$$= \mathbf{B}^{\mathrm{H}}\left(\mathrm{I} + \mathbf{V}_M\mathbf{D}_M\mathbf{U}_M^{\mathrm{H}}\mathbf{U}_M\mathbf{D}_M\mathbf{V}_M^{\mathrm{H}}\right)^{-1}\mathbf{B}$$

$$= \mathbf{B}^{\mathrm{H}}\left(\mathbf{I} + \mathbf{V}_M\mathbf{D}_M^2\mathbf{V}_M^{\mathrm{H}}\right)^{-1}\mathbf{B}$$

$$= \mathbf{B}^{\mathrm{H}}\left(\mathbf{V}_M\mathbf{V}_M^{\mathrm{H}} + \mathbf{V}_M\mathbf{D}_M^2\mathbf{V}_M^{\mathrm{H}}\right)^{-1}\mathbf{B}$$

$$= \mathbf{B}^{\mathrm{H}}\left(\mathbf{V}_M(\mathbf{I} + \mathbf{D}_M^2)\mathbf{V}_M^{\mathrm{H}}\right)^{-1}\mathbf{B}$$

$$= \mathbf{B}^{\mathrm{H}}(\mathbf{V}_M^{-\mathrm{H}}\left(\mathbf{I} + \mathbf{D}_M^2\right)^{-1}\mathbf{V}_M^{-1})\mathbf{B}$$

$$= \mathbf{B}^{\mathrm{H}}(\mathbf{V}_{\mathrm{M}}\left(\mathbf{I}+\mathbf{D}_{\mathrm{M}}^{2}\right)^{-1}\mathbf{V}_{\mathrm{M}}^{\mathrm{H}})\mathbf{B} \tag{4.12}$$

In the derivation above, we have used the properties of a unitary matrix, such as $\mathbf{V}_{\mathrm{M}}\mathbf{V}_{\mathrm{M}}^{\mathrm{H}}=\mathbf{I}$ and $\mathbf{V}_{\mathrm{M}}^{-1}=\mathbf{V}_{\mathrm{M}}^{\mathrm{H}}$.

We may perform SVD to factorize the M-by-M Hermitian matrix $\mathbf{V}_{\mathrm{M}}\left(\mathbf{I}+\mathbf{D}_{\mathrm{M}}^{2}\right)^{-1}\mathbf{V}_{\mathrm{M}}^{\mathrm{H}}$ in (4.12) into $\mathbf{W}_{\mathrm{M}}\mathbf{\Sigma}\mathbf{W}_{\mathrm{M}}^{\mathrm{H}}$, where $\mathbf{W}_{\mathrm{M}}$ is a M-by-M unitary matrix and $\mathbf{\Sigma}$ is a M-by-M diagonal matrix. We know that the diagonal matrix $\mathbf{\Sigma}$ is uniquely determined, but the unitary matrix $\mathbf{W}_{\mathrm{M}}$ is not necessarily unique [41]; that is, one SVD factorization can be $\mathbf{V}_{\mathrm{M}}\mathbf{\Sigma}\mathbf{V}_{\mathrm{M}}^{\mathrm{H}}$ with $\mathbf{\Sigma}=\left(\mathbf{I}+\mathbf{D}_{\mathrm{M}}^{2}\right)^{-1}$ and another factorization can be $\mathbf{W}_{\mathrm{M}}\mathbf{\Sigma}\mathbf{W}_{\mathrm{M}}^{\mathrm{H}}$. Since diagonal entries in $\mathbf{D}_{\mathrm{M}}$ are arranged in descending order, diagonal entries in $\mathbf{\Sigma}$ are in ascending order. Theorem 3.1.1' in [41] can be utilized to find relationship between $\mathbf{V}_{\mathrm{M}}$ and $\mathbf{W}_{\mathrm{M}}$. In particular, with the fact that SVD is performed on a Hermitian matrix $\mathbf{V}_{\mathrm{M}}\left(\mathbf{I}+\mathbf{D}_{\mathrm{M}}^{2}\right)^{-1}\mathbf{V}_{\mathrm{M}}^{\mathrm{H}}$ and the rank is r (because $\mathbf{D}_{\mathrm{M}}$ consists of r positive values and M-r zeros along its diagonal), The resulting $\mathbf{W}_{\mathrm{M}}$ can be simplified as $\mathbf{W}_{\mathrm{M}}=\mathbf{V}_{\mathrm{M}}[\mathbf{U}_1\oplus\cdots\oplus\mathbf{U}_{\mathrm{k}}\oplus\mathbf{U}_{\mathrm{k+1}}]$**,** where $\oplus$ denotes direct sum and $\mathbf{U}_{\mathrm{i}}$ is a $\mu_{\mathrm{i}}$-by-$\mu_{\mathrm{i}}$ unitary matrix with $\mu_1+\ldots+\mu_{\mathrm{k}}=\mathrm{r}$ and $\mu_{\mathrm{k+1}}=\mathrm{M-r}$. These $\mu_{\mathrm{i}}$ values represent the multiplicities of the singular values. For example, when all singular values are different, all $\mu_{\mathrm{i}}$ values are unity.

Previously we have known that the optimum $\mathbf{B}_{\mathrm{opt}}$ consists of r eigenvectors corresponding to the r smallest eigenvalues of $\mathbf{R}_{\mathrm{aa}}-\mathbf{R}_{\mathrm{ay}}\mathbf{R}_{\mathrm{yy}}^{-1}\mathbf{R}_{\mathrm{ya}}$. Now we see that this matrix is equal to $\mathbf{V}_{\mathrm{M}}\left(\mathbf{I}+\mathbf{D}_{\mathrm{M}}^{2}\right)^{-1}\mathbf{V}_{\mathrm{M}}^{\mathrm{H}}$, whose eigenvalues are the diagonal entries in $\left(\mathbf{I}+\mathbf{D}_{\mathrm{M}}^{2}\right)^{-1}$ arranged in ascending order and whose SVD factorization is $\mathbf{W}_{\mathrm{M}}\mathbf{\Sigma}\mathbf{W}_{\mathrm{M}}^{\mathrm{H}}$ with $\mathbf{\Sigma}=\left(\mathbf{I}+\mathbf{D}_{\mathrm{M}}^{2}\right)^{-1}$. Hence, the resulting $\mathbf{B}_{\mathrm{opt}}$, by minimizing trace($\mathbf{R}_{\mathrm{ee}}$), consists of the first r vectors in the unitary matrix $\mathbf{W}_{\mathrm{M}}$ and can be expressed as $\mathbf{B}_{\mathrm{opt}}=\mathbf{V}_{\mathrm{r}}[\mathbf{U}_1\oplus\cdots\oplus\mathbf{U}_{\mathrm{k}}]$. Meanwhile, the resulting autocorrelation of the noise vector becomes

$$\mathbf{R}_{\mathrm{ee,min}}=(\mathbf{I}+\mathbf{D}_{\mathrm{r}}^{2})^{-1} \tag{4.13}$$

where $\mathbf{D}_{\mathrm{r}}$ is a r-by-r diagonal matrix whose diagonal entries are the first r diagonal entries in $\mathbf{D}_{\mathrm{M}}$.

Additionally, an important fact worth mentioning is that $[\mathbf{U}_1\oplus\cdots\oplus\mathbf{U}_{\mathrm{k}}][\mathbf{U}_1\oplus\cdots\oplus\mathbf{U}_{\mathrm{k}}]^{\mathrm{H}}=\mathbf{I}$, which can be justified easily by considering the unitary submatrix $\mathbf{U}_{\mathrm{i}}$ in $[\mathbf{U}_1\oplus\cdots\oplus\mathbf{U}_{\mathrm{k}}]$**.** This fact will be used near the end of the proof.

It is known that linear or widely linear MMSE filters minimize the MSE but are biased estimators [39]. Hence, the actual post-filter CIR matrix is not equal to $\mathbf{B}_{\text{opt}}^{\text{H}}$. Assume the MMSE filter is $\mathbf{F} = \mathbf{R}_{\text{yy}}^{-1}\mathbf{R}_{\text{ya}}\mathbf{B}_{\text{opt}}$, the actual post-filter CIR is

$$\begin{aligned}\mathbf{B}_{\text{actual}}^{\text{H}} &= \mathbf{F}^{\text{H}}\mathbf{H} \\ &= \mathbf{B}_{\text{opt}}^{\text{H}}\mathbf{R}_{\text{ay}}\mathbf{R}_{\text{yy}}^{-1}\mathbf{H} \\ &= \mathbf{B}_{\text{opt}}^{\text{H}}\mathbf{H}^{\text{H}}\mathbf{R}_{\text{yy}}^{-1}\mathbf{H}\end{aligned} \tag{4.14}$$

where the last line is due to the fact that $\mathbf{R}_{\text{ya}}$ is equal to the CIR matrix $\mathbf{H}$ when $\mathbf{R}_{\text{aa}}$ is an identity matrix; hence, $\mathbf{R}_{\text{ay}}$ is equal to $\mathbf{H}^{\text{H}}$.

We know that

$$\begin{aligned}\mathbf{R}_{\text{ee,min}} &= \mathbf{B}_{\text{opt}}^{\text{H}}\left(\mathbf{R}_{\text{aa}} - \mathbf{R}_{\text{ay}}\mathbf{R}_{\text{yy}}^{-1}\mathbf{R}_{\text{ya}}\right)\mathbf{B}_{\text{opt}} \\ &= \mathbf{B}_{\text{opt}}^{\text{H}}\mathbf{R}_{\text{aa}}\mathbf{B}_{\text{opt}} - \mathbf{B}_{\text{opt}}^{\text{H}}\mathbf{R}_{\text{ay}}\mathbf{R}_{\text{yy}}^{-1}\mathbf{R}_{\text{ya}}\mathbf{B}_{\text{opt}} \\ &= \mathbf{I} - \mathbf{B}_{\text{opt}}^{\text{H}}\mathbf{H}^{\text{H}}\mathbf{R}_{\text{yy}}^{-1}\mathbf{H}\mathbf{B}_{\text{opt}}\end{aligned} \tag{4.15}$$

Substitute $\mathbf{B}_{\text{actual}}^{\text{H}} = \mathbf{B}_{\text{opt}}^{\text{H}}\mathbf{H}^{\text{H}}\mathbf{R}_{\text{yy}}^{-1}\mathbf{H}$ from (4.14) into (4.15), we have $\mathbf{R}_{\text{ee,min}} = \mathbf{I} - \mathbf{B}_{\text{actual}}^{\text{H}}\mathbf{B}_{\text{opt}}$, or

$$\begin{aligned}\mathbf{B}_{\text{actual}}^{\text{H}} &= \left(\mathbf{I} - \mathbf{R}_{\text{ee,min}}\right)\mathbf{B}_{\text{opt}}^{\text{H}} \\ &= (\mathbf{I} - (\mathbf{I} + \mathbf{D}_{\text{r}}^2)^{-1})\mathbf{B}_{\text{opt}}^{\text{H}} \\ &= \mathbf{D}_{\text{r}}^2(\mathbf{I} + \mathbf{D}_{\text{r}}^2)^{-1}\mathbf{B}_{\text{opt}}^{\text{H}}\end{aligned} \tag{4.16}$$

After finding the post-filter TIR matrix $\mathbf{B}_{\text{actual}}^{\text{H}}$, let us find the actual unbiased MSE $\mathbf{R}_{\text{ee,actual}}$ at the MMSE filter output. We know that $\mathbf{R}_{\text{ee,actual}} = \mathbf{F}^{\text{H}}\mathbf{R}_{\text{nn}}\mathbf{F}$. Let us decompose $\mathbf{F}$ first.

$$\begin{aligned}\mathbf{F} &= \mathbf{R}_{\text{yy}}^{-1}\mathbf{R}_{\text{ya}}\mathbf{B}_{\text{opt}} \\ &= (\mathbf{H}\mathbf{R}_{\text{aa}}\mathbf{H}^{\text{H}} + \mathbf{R}_{\text{nn}})^{-1}\mathbf{H}\mathbf{B}_{\text{opt}} \\ &= (\mathbf{H}\mathbf{H}^{\text{H}} + \mathbf{R}_{\text{nn}})^{-1}\mathbf{H}\mathbf{B}_{\text{opt}} \\ &= (\mathbf{R}_{\text{nn}}^{-1} - \mathbf{R}_{\text{nn}}^{-1}\mathbf{H}\left(\mathbf{I} + \mathbf{H}^{\text{H}}\mathbf{R}_{\text{nn}}^{-1}\mathbf{H}\right)^{-1}\mathbf{H}^{\text{H}}\mathbf{R}_{\text{nn}}^{-1})\mathbf{H}\mathbf{B}_{\text{opt}} \\ &= \mathbf{R}_{\text{nn}}^{-\text{H}/2}(\mathbf{R}_{\text{nn}}^{-1/2}\mathbf{H}\mathbf{B}_{\text{opt}} - \mathbf{R}_{\text{nn}}^{-1/2}\mathbf{H}\left(\mathbf{I} + \mathbf{H}^{\text{H}}\mathbf{R}_{\text{nn}}^{-\text{H}/2}\mathbf{R}_{\text{nn}}^{-1/2}\mathbf{H}\right)^{-1}\mathbf{H}^{\text{H}}\mathbf{R}_{\text{nn}}^{-\text{H}/2}\mathbf{R}_{\text{nn}}^{-1/2}\mathbf{H}\mathbf{B}_{\text{opt}})\end{aligned} \tag{4.17}$$

Since it has been found that $\mathbf{B}_{\text{opt}} = \mathbf{V}_{\text{r}}[\mathbf{U}_1 \oplus \cdots \oplus \mathbf{U}_{\text{k}}]$ and $\mathbf{H}_{\text{NW}} = \mathbf{R}_{\text{nn}}^{-1/2}\mathbf{H} = \mathbf{U}_{\text{r}}\mathbf{D}_{\text{r}}\mathbf{V}_{\text{r}}^{\text{H}}$, we have

$$\mathbf{F} = \mathbf{R}_{\text{nn}}^{-\text{H}/2}(\mathbf{U}_{\text{r}}\mathbf{D}_{\text{r}}\mathbf{V}_{\text{r}}^{\text{H}}\mathbf{B}_{\text{opt}} - \mathbf{U}_{\text{r}}\mathbf{D}_{\text{r}}\mathbf{V}_{\text{r}}^{\text{H}}\left(\mathbf{I} + \mathbf{V}_{\text{r}}\mathbf{D}_{\text{r}}\mathbf{U}_{\text{r}}{}^{\text{H}}\mathbf{U}_{\text{r}}\mathbf{D}_{\text{r}}\mathbf{V}_{\text{r}}^{\text{H}}\right)^{-1}\mathbf{V}_{\text{r}}\mathbf{D}_{\text{r}}\mathbf{U}_{\text{r}}{}^{\text{H}}\mathbf{U}_{\text{r}}\mathbf{D}_{\text{r}}\mathbf{V}_{\text{r}}^{\text{H}}\mathbf{B}_{\text{opt}})$$

$$= \mathbf{R}_{\text{nn}}^{-\text{H}/2}(\mathbf{U}_{\text{r}}\mathbf{D}_{\text{r}}[\mathbf{U}_1 \oplus \cdots \oplus \mathbf{U}_{\text{k}}] - \mathbf{U}_{\text{r}}\mathbf{D}_{\text{r}}\mathbf{V}_{\text{r}}^{\text{H}}\left(\mathbf{I} + \mathbf{V}_{\text{r}}\mathbf{D}_{\text{r}}^2\mathbf{V}_{\text{r}}^{\text{H}}\right)^{-1}\mathbf{V}_{\text{r}}\mathbf{D}_{\text{r}}^2[\mathbf{U}_1 \oplus \cdots \oplus \mathbf{U}_{\text{k}}])$$

$$= \mathbf{R}_{\text{nn}}^{-\text{H}/2}\mathbf{U}_{\text{r}}\mathbf{D}_{\text{r}}(\mathbf{I} - \mathbf{V}_{\text{r}}^{\text{H}}\left(\text{I} + \mathbf{V}_{\text{r}}\mathbf{D}_{\text{r}}^2\mathbf{V}_{\text{r}}^{\text{H}}\right)^{-1}\mathbf{V}_{\text{r}}\mathbf{D}_{\text{r}}^2)[\mathbf{U}_1 \oplus \cdots \oplus \mathbf{U}_{\text{k}}]$$

$$= \mathbf{R}_{\text{nn}}^{-\text{H}/2}\mathbf{U}_{\text{r}}\mathbf{D}_{\text{r}}(\mathbf{I} + \mathbf{V}_{\text{r}}^{\text{H}}\mathbf{V}_{\text{r}}\mathbf{D}_{\text{r}}^2)^{-1}[\mathbf{U}_1 \oplus \cdots \oplus \mathbf{U}_{\text{k}}]$$

$$= \mathbf{R}_{\text{nn}}^{-\text{H}/2}\mathbf{U}_{\text{r}}\mathbf{D}_{\text{r}}(\mathbf{I} + \mathbf{D}_{\text{r}}^2)^{-1}[\mathbf{U}_1 \oplus \cdots \oplus \mathbf{U}_{\text{k}}] \tag{4.18}$$

Hence,

$$\mathbf{R}_{\text{ee,actual}} = \mathbf{F}^{\text{H}}\mathbf{R}_{\text{nn}}\mathbf{F}$$

$$= (\mathbf{F}^{\text{H}}\text{R}_{\text{nn}}^{\text{H}/2})(\mathbf{R}_{\text{nn}}^{1/2}\mathbf{F})$$

$$= ([\mathbf{U}_1 \oplus \cdots \oplus \mathbf{U}_{\text{k}}]^{\text{H}}\mathbf{D}_{\text{r}}(\mathbf{I} + \mathbf{D}_{\text{r}}^2)^{-1}\mathbf{U}_{\text{r}}^{\text{H}}\mathbf{R}_{\text{nn}}^{-1/2}\mathbf{R}_{\text{nn}}^{\text{H}/2})(\mathbf{R}_{\text{nn}}^{1/2}\mathbf{R}_{\text{nn}}^{-\text{H}/2}\mathbf{U}_{\text{r}}\mathbf{D}_{\text{r}}(\mathbf{I} + \mathbf{D}_{\text{r}}^2)^{-1}[\mathbf{U}_1 \oplus \cdots \oplus \mathbf{U}_{\text{k}}])$$

$$= [\mathbf{U}_1 \oplus \cdots \oplus \mathbf{U}_{\text{k}}]^{\text{H}}(\mathbf{D}_{\text{r}}(\mathbf{I} + \mathbf{D}_{\text{r}}^2)^{-1}\mathbf{U}_{\text{r}}^{\text{H}}\mathbf{U}_{\text{r}}\mathbf{D}_{\text{r}}(\mathbf{I} + \mathbf{D}_{\text{r}}^2)^{-1})[\mathbf{U}_1 \oplus \cdots \oplus \mathbf{U}_{\text{k}}]$$

$$= [\mathbf{U}_1 \oplus \cdots \oplus \mathbf{U}_{\text{k}}]^{\text{H}}\mathbf{D}_{\text{r}}^2(\mathbf{I} + \mathbf{D}_{\text{r}}^2)^{-2}[\mathbf{U}_1 \oplus \cdots \oplus \mathbf{U}_{\text{k}}] \tag{4.19}$$

With this resulting $\mathbf{R}_{\text{ee,actual}}$, the noise whitening filter is $[\mathbf{U}_1 \oplus \cdots \oplus \mathbf{U}_{\text{k}}]^{\text{H}}\mathbf{D}_{\text{r}}^{-1}(\mathbf{I} + \mathbf{D}_{\text{r}}^2)$. By cascading this filter with the MMSE filter $\mathbf{F}$, the overall filter becomes

$$\mathbf{F}_{\text{overall}} = [\mathbf{U}_1 \oplus \cdots \oplus \mathbf{U}_{\text{k}}]^{\text{H}}\mathbf{D}_{\text{r}}^{-1}(\mathbf{I} + \mathbf{D}_{\text{r}}^2)\mathbf{F}^{\text{H}}$$

$$= [\mathbf{U}_1 \oplus \cdots \oplus \mathbf{U}_{\text{k}}]^{\text{H}}\mathbf{D}_{\text{r}}^{-1}(\mathbf{I} + \mathbf{D}_{\text{r}}^2)\mathbf{D}_{\text{r}}(\mathbf{I} + \mathbf{D}_{\text{r}}^2)^{-1}\mathbf{U}_{\text{r}}^{\text{H}}\mathbf{R}_{\text{nn}}^{-1/2}$$

$$= [\mathbf{U}_1 \oplus \cdots \oplus \mathbf{U}_{\text{k}}]^{\text{H}}\mathbf{U}_{\text{r}}^{\text{H}}\mathbf{R}_{\text{nn}}^{-1/2} \tag{4.20}$$

Meanwhile, the overall post-filter CIR becomes

$$\mathbf{B}_{\text{overall}}^{\text{H}} = \mathbf{F}_{\text{overall}}\mathbf{H}$$

$$\mathbf{B}_{\text{overall}}^{\text{H}} = [\mathbf{U}_1 \oplus \cdots \oplus \mathbf{U}_{\text{k}}]^{\text{H}}\mathbf{U}_{\text{r}}^{\text{H}}\mathbf{R}_{\text{nn}}^{-1/2}\mathbf{H}$$

$$\mathbf{B}_{\text{overall}}^{\text{H}} = [\mathbf{U}_1 \oplus \cdots \oplus \mathbf{U}_{\text{k}}]^{\text{H}}\mathbf{U}_{\text{r}}^{\text{H}}\mathbf{H}_{\text{NW}}$$

$$\mathbf{B}_{\text{overall}}^{\text{H}} = [\mathbf{U}_1 \oplus \cdots \oplus \mathbf{U}_{\text{k}}]^{\text{H}}\mathbf{U}_{\text{r}}^{\text{H}}\mathbf{U}_{\text{r}}\mathbf{D}_{\text{r}}\mathbf{V}_{\text{r}}^{\text{H}}$$

$$\mathbf{B}_{\text{overall}}^{\text{H}} = [\mathbf{U}_1 \oplus \cdots \oplus \mathbf{U}_{\text{k}}]^{\text{H}} \mathbf{D}_{\text{r}} \mathbf{V}_{\text{r}}^{\text{H}} \tag{4.21}$$

Hence, the Euclidean-distance branch metric in the MLSE stage is

$$\text{L}_2\{\mathbf{a}_{\text{M}}(\text{k})\} = \left\| \mathbf{F}_{\text{overall}} \mathbf{y}_{\text{N}}(\text{k}) - \mathbf{B}_{\text{overall}}^{\text{H}} \mathbf{a}_{\text{M}}(\text{k}) \right\|^2$$

$$= \left\| [\mathbf{U}_1 \oplus \cdots \oplus \mathbf{U}_{\text{k}}]^{\text{H}} \mathbf{U}_{\text{r}}^{\text{H}} \mathbf{R}_{\text{nn}}^{-1/2} \mathbf{y}_{\text{N}}(\text{k}) - [\mathbf{U}_1 \oplus \cdots \oplus \mathbf{U}_{\text{k}}]^{\text{H}} \mathbf{D}_{\text{r}} \mathbf{V}_{\text{r}}^{\text{H}} \mathbf{a}_{\text{M}}(\text{k}) \right\|^2$$

$$= \left\| [\mathbf{U}_1 \oplus \cdots \oplus \mathbf{U}_{\text{k}}]^{\text{H}} \left( \mathbf{U}_{\text{r}}^{\text{H}} \mathbf{R}_{\text{nn}}^{-1/2} \mathbf{y}_{\text{N}}(\text{k}) - \mathbf{D}_{\text{r}} \mathbf{V}_{\text{r}}^{\text{H}} \mathbf{a}_{\text{M}}(\text{k}) \right) \right\|^2$$

$$= \left( \mathbf{U}_{\text{r}}^{\text{H}} \mathbf{R}_{\text{nn}}^{-1/2} \mathbf{y}_{\text{N}}(\text{k}) - \mathbf{D}_{\text{r}} \mathbf{V}_{\text{r}}^{\text{H}} \mathbf{a}_{\text{M}}(\text{k}) \right)^{\text{H}} [\mathbf{U}_1 \oplus \cdots \oplus \mathbf{U}_{\text{k}}][\mathbf{U}_1 \oplus \cdots \oplus \mathbf{U}_{\text{k}}]^{\text{H}} \left( \mathbf{U}_{\text{r}}^{\text{H}} \mathbf{R}_{\text{nn}}^{-1/2} \mathbf{y}_{\text{N}}(\text{k}) - \right.$$

$\left. \mathbf{D}_{\text{r}} \mathbf{V}_{\text{r}}^{\text{H}} \mathbf{a}_{\text{M}}(\text{k}) \right)$

$$= \left( \mathbf{U}_{\text{r}}^{\text{H}} \mathbf{R}_{\text{nn}}^{-1/2} \mathbf{y}_{\text{N}}(\text{k}) - \mathbf{D}_{\text{r}} \mathbf{V}_{\text{r}}^{\text{H}} \mathbf{a}_{\text{M}}(\text{k}) \right)^{\text{H}} \left( \mathbf{U}_{\text{r}}^{\text{H}} \mathbf{R}_{\text{nn}}^{-1/2} \mathbf{y}_{\text{N}}(\text{k}) - \mathbf{D}_{\text{r}} \mathbf{V}_{\text{r}}^{\text{H}} \mathbf{a}_{\text{M}}(\text{k}) \right)$$

$$= \left\| \mathbf{U}_{\text{r}}^{\text{H}} \mathbf{R}_{\text{nn}}^{-1/2} \mathbf{y}_{\text{N}}(\text{k}) - \mathbf{D}_{\text{r}} \mathbf{V}_{\text{r}}^{\text{H}} \mathbf{a}_{\text{M}}(\text{k}) \right\|^2 \tag{4.22}$$

where we have used the fact that $[\mathbf{U}_1 \oplus \cdots \oplus \mathbf{U}_{\text{k}}][\mathbf{U}_1 \oplus \cdots \oplus \mathbf{U}_{\text{k}}]^{\text{H}} = \mathbf{I}$, as mentioned previously.

Now we obtain the desired result that the branch metric $\text{L}_2\{\mathbf{a}_{\text{M}}(\text{k})\}$ of the MMSE filter based MLSE in (4.22) is equal to the branch metric $\text{L}_1\{\mathbf{a}_{\text{M}}(\text{k})\}$ of the modified noise whitening filter based MLSE in (4.10). Since (4.9) and (4.10) have proved the equivalence between the standard noise whitening filter based MLSE and the modified noise whitening filter based MLSE, we now have proved that all three forms of MLSE equalizers are equivalent. ■

The equivalence of the three MLSE equalizers is depicted as below.

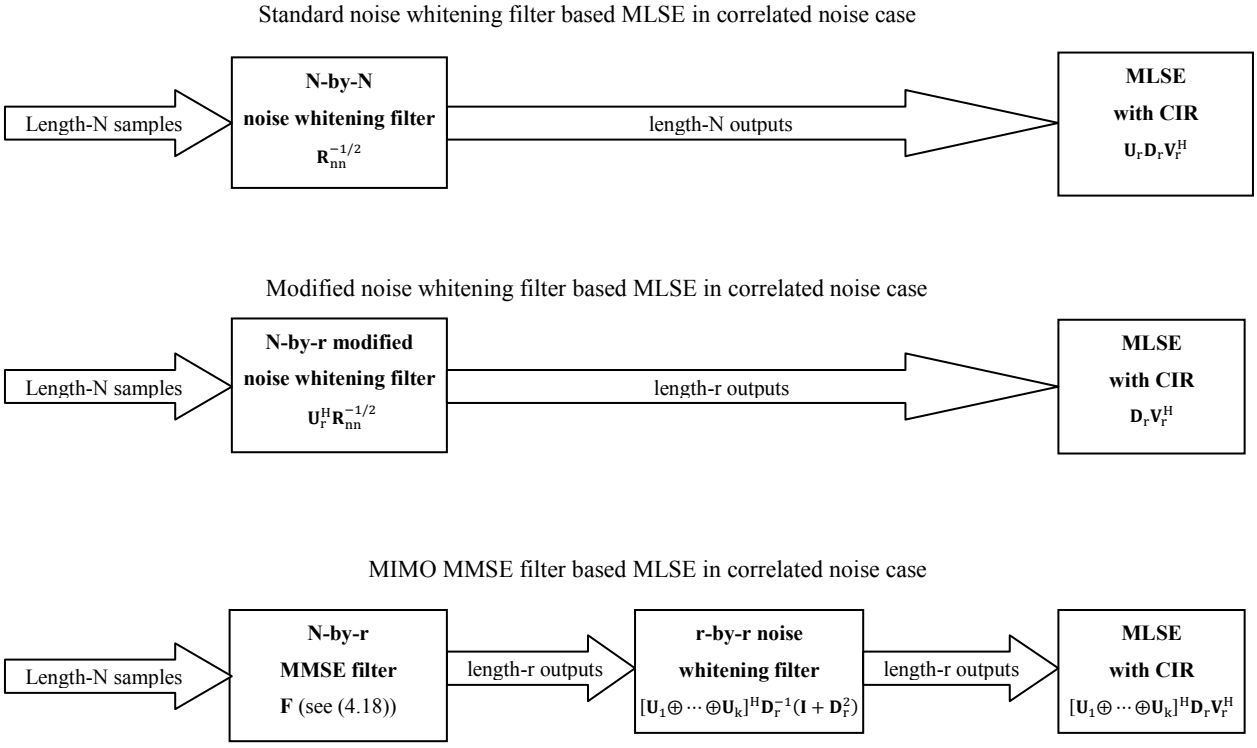


**Figure 4.3 Equivalence between MMSE filter based and noise whitening filter based equalizers with the rank r channel model**

# Chapter 5
# Simulation results of various equalizers in VAMOS test scenarios

Comprehensive simulation results are provided in this chapter to compare various equalizers in different VAMOS test scenarios. The purpose of the simulation work is to justify that the proposed reduced rank widely linear MIMO MMSE filter based JMLSE equalizer is superior to other equalizers in most VAMOS test scenarios. The first section describes the simulation environment and the second section reports simulation results.

## 5.1 Simulation environment

The first subsection below defines the abbreviated names and descrbes the comparing equalizers, and the second subsection clarifies the simulation parameters of the transmitter, the receiver, the fading channel, and the interferer.

### 5.1.1 Abbreviated names and description of the comparing equalizers

Simulation in this chapter attempts to find the benefits of widely linear processing and JMLSE in the proposed equalizer. This equalizer consists of a widely linear MIMO MMSE filter and 2-user JMLSE; hence, abbreviated as WLMMSE-2UML.

In order to obtain fair companion, two of the comparing equalizers differ from the proposed solution by only one component, rspectively. One equalizer consists of a linear MMSE filter and 2-user JMLSE, named as LMMSE-2UML; the other one contains a widely linear MMSE filter and single-user MLSE, named as WLMMSE-1UML. This equalizer is similar to the space-time data model based equalizer in [8] (described in subsection 3.1.2), except that we extend the filter into a widely linear form.

We also attempt to compare recent years' VAMOS solutions but with some adaptation in order to simplify simulation work. VAMOS is a new transmission scheme so that not many solutions are proposed for this operating mode except the ones in [20] and [42]. The VAMOS equalizer in [20] is based on the VAR disturbance model [21] (described in subsection 3.1.3), and simulation results in [11] (described in subsection 3.1.4) have shown that it is inferior to the STBD equalizer proposed in that publication. Therefore, a widely linear noise whitening filter based JMLSE equalizer equivalent to the STBD equalizer (different only in the branch metric calculation of JMLSE but giving the same output sequence) is included in simulation. It is named as WLNW-2UML. The other VAMOS

equalizer [42] is not tested because it falls into the adaptive equalization category (the MMSE filter coefficients are iteratively calculated based on the least mean square, or LMS, adaptive filtering algorithm).

In order to justify the optimality of the MSE criterion, simulation comparison also includes a recent widely linear equalizer from [13] (described in subsection 3.1.5), in which the widely linear filter attempts to maximize the filter output signal to interference ratio (SIR). It is named as WLMSIR-1UML. Since the widely linear MMSE filter in our work is equivalent to a max-SINR filter (which maximizes the filter output SINR), it is expected that WLMMSE-1UML (as well as WLMMSE-2UML) outperforms WLMSIR-1UML in interference plus noise scenarios.

During simulation, it was found that when $\alpha<1$ (denoting that downlink signal in the desired user's subchannel is weaker than the paired user's subchannel), the widely linear MMSE filter based JMLSE is inferior to the linear MMSE filter based JMLSE. Explanation will be given where the corresponding simulation results are presented. In order to overcome this problem, a solution named WLMMSE-2UMLBS is proposed to augment WLMMSE-2UML with a bootstrap method [1]. Specifically, this equalizer performs the same filtering and JMLSE processing as WLMMSE-2UML first. Then, as a threshold, if the energy of the paired user in the resulting post-filter CIR is greater than that of the desired user, BER of the paired user's detected sequence is expected to be lower than that of the desired user. In this case, contribution of the paired user to the received samples is reconstructed based on the paired user's detected sequence and estimated CIR, and removed from the received samples. Then, single-user equalization w.r.t. the desired user is followed to detect the desired user's sequence. This equalizer yields better BER than the original WLMMSE-2UML when $\alpha<1$.

### 5.1.2 Parameters of each components in the test system

In the simulation, we test different transmitter sub-channel power imbalance ratios (SCPIR). In particular, we follow 3GPP technical document [43] to select $\alpha$ values of 1.3, 1, or 0.54, corresponding to SCPIR 7.7 dB (downlink signal in the desired user's subchannel is 7.7 dB stronger than the other subchannel), 0 dB (equal power levels in both subchannels), or -7.7 dB (downlink signal in the desired user's subchannel is 7.7 dB weaker than the other subchannel), respectively.

On the receiver side, 2x oversampling is used. To simplify the problem formulation, we omit the channel selection filter and assume the noise part of the disturbance is AWGN. The augmented

received sample vectors are formed by stacking received samples from 2 temporally adjacent symbol periods (that is, 4 samples from 2 symbol periods due to 2x oversampling). A larger-size augmented received sample vector typically makes the filter more effective to suppress interference. However, the resulting residue disturbance at the filter output becomes more temporally correlated because more adjacent augmented received sample vectors contain common received samples. In order to utilize an existing JMLSE whose input is complex-valued scalar or real-valued length-2 vectors, the WLMMSE-2UML and WLNW-2UML equalizers have 2 real-valued outputs and other equalizers have one complex-valued or real-valued output. Not only to simplify simulation work, the rank-one or rank-two channel model and corresponding equalizers are a practical approach to combat channel estimation inaccuracy and accommodate high correlation among different virtual channels. Several GSM interference cancellation publications such as [33] have found that in field trials the rank-one equalizer is almost as good as equalizers with less rank reduction.

For temporal CIR length, we select L=4 symbol periods. As we have mentioned before, the transmitter LGMSK pulse spans 3 symbol periods, and the typical urban fading channel extends the overall CIR by one more symbol period approximately. The radio channel tested with is typical urban 3km (TU3) profile, which is the most commonly used channel model in many GSM or VAMOS interference cancellation publications.

For the VAMOS interferer, we test different $\alpha$ values of 1.3, 1, or 0.54, respectively.

For the test system in general, 100 iterations run for each test point. In noise-limited test scenarios, we have AWGN noise only; while in interference-limited scenarios, we include a -15 dB (w.r.t the VAMOS signal containing the desired user) AWGN noise besides the VAMOS interferer.

For the BER range of interest, we focus on 2%-20% as this range reflects the FER range of most channel coding schemes. That is, when BER is below 0.02, FER of all channel coding schemes approaches zero; when BER is above 0.2, BER of all channel coding schemes are greater than 0.1, which is beyond the interested range of channel coding. A figure from [3] is duplicated below to confirm this fact.

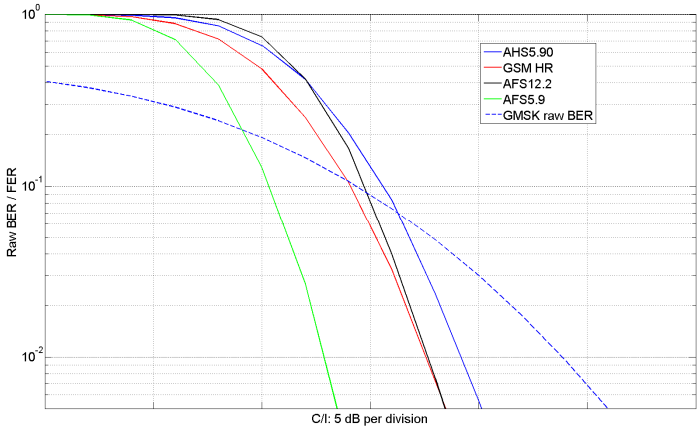


**Figure 5.1 Raw BER vs. FER for different speech codecs, duplicated from** [3]

In the simulation results in the following section, each figure consists of two subplots, one for the filter output SINR, and the other showing the equalizer output BER.

## 5.2 Performance of different equalizers

In the first subsection, we present the simulation results of WLMMSE-2UML and WLNW-2UML to confirm their equivalence, in order to justify the proof in section 4.2. In the second subsection, WLMMSE-1UML and WLMSIR-1UML are tested to justify the superiority of our MMSE filter w.r.t. the maximum SIR optimization algorithm [13] in interference plus noise scenarios. In the rest subsections, we then exclude WLNW-2UML (which is equivalent to WLMMSE-2UML) and WLMSIR-1UML (which is inferior to WLMMSE-1UML) and focus on other equalizers to find the performance gain of the proposed WLMMSE-2UML equalizer w.r.t. comparing equalizers in different VAMOS test scenarios.

### 5.2.1 The comparison of WLMMSE-2UML and WLNW-2UML in the known second order statistics case

As proved in section 4.2, when the second order statistics are known, WLMMSE-2UML and WLNW-2UML are fully equivalent. Two simulation figures below confirm the theoretical proof. One figure is for $\alpha$=1.3 in the noise-limited scenario; the other one is for $\alpha$=1 in the interference-limited case. Results in other test scenarios are expected to be the same but omitted.

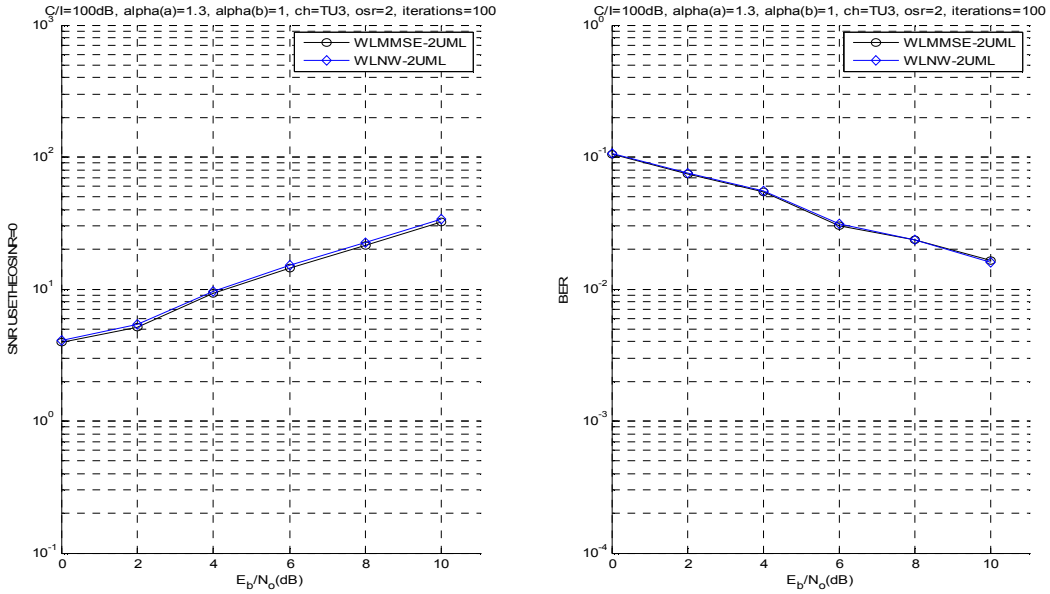


**Figure 5.2 Equivalence between MMSE filter and noise whitening filter based equalizers in a noise-limited scenario**

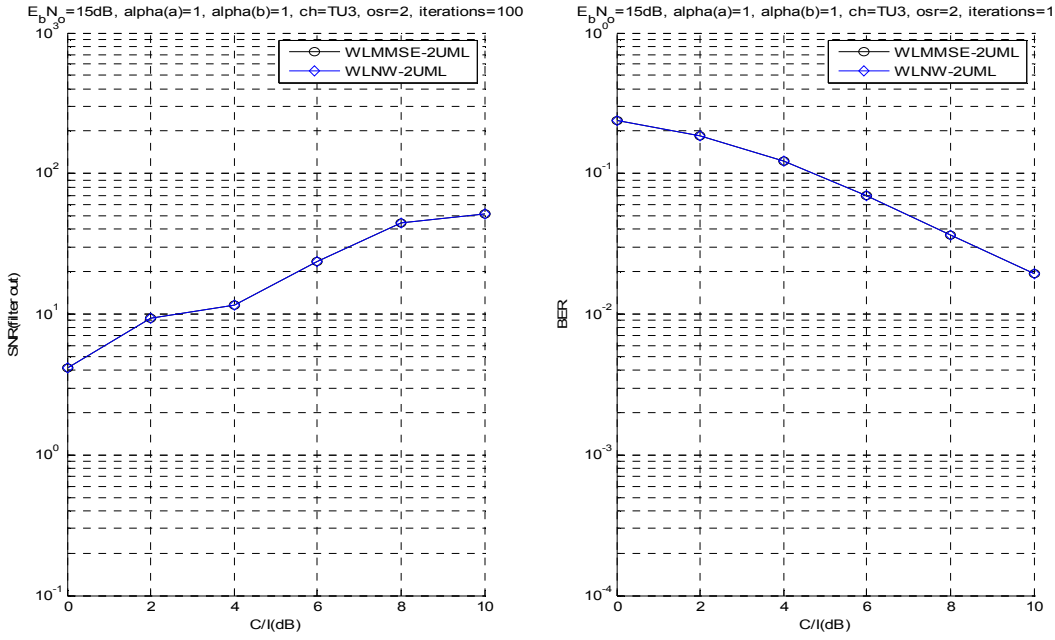


**Figure 5.3 Equivalence between MMSE filter and noise whitening filter based equalizers in an interference-limited scenario**

### 5.2.2 WLMMSE-1UML yields better performance than WLMSIR-1UML in interference plus noise scenarios

It is intuitive that in interference plus noise scenarios, it is optimum for the filter to suppress interference plus noise, instead of only rejecting the interference. The figure below confirms this expectation by two equalizers, WLMMSE-1UML whose MMSE filter is equivalent to a filter maximizing filter output SINR, and WLMSIR-1UML which attempts to maximize SIR in the filtering stage. The AWGN noise in this test scenario is fixed to be 15 dB lower than the VAMOS signal containing the desired user.

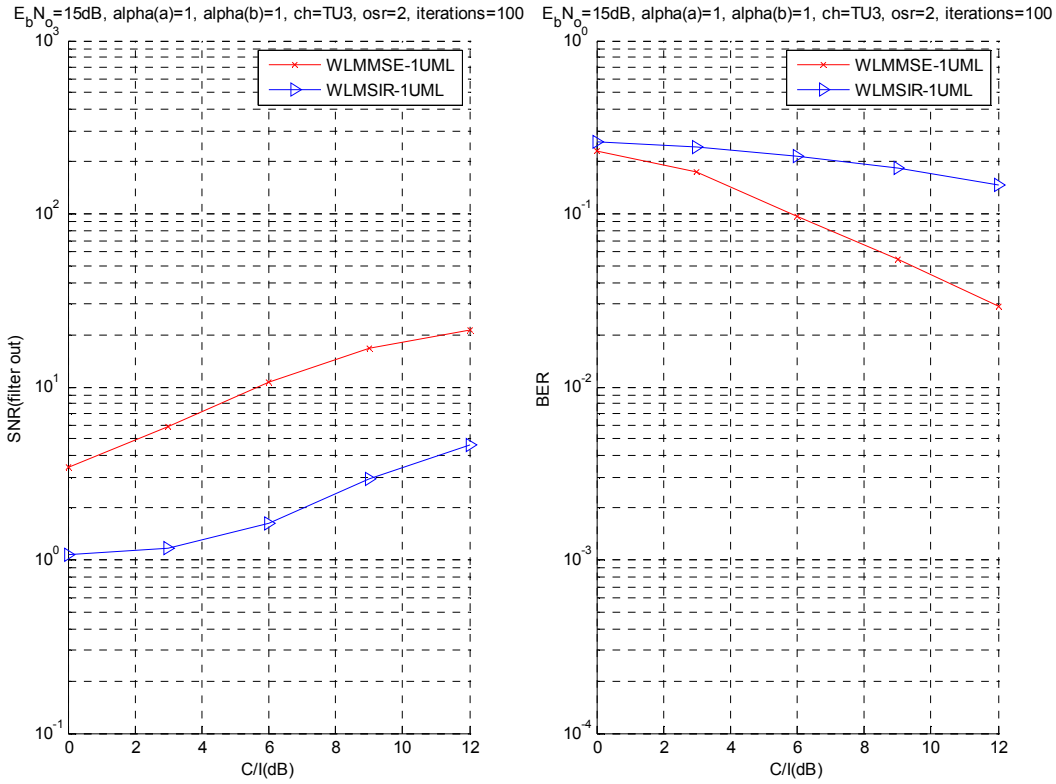


**Figure 5.4 WLMMSE-1UML yields better performance than WLMSIR-1UML in interference plus noise scenarios**

### 5.2.3 Performance in the noise-limited test scenario with α=1

Since in this scenario the transmitted signal and the received signal are jointly proper, we expect WLMMSE-2UML and LMMSE-2UML perform equally well, and WLMMSE-1UML performs the worst. The figure below confirms this expectation in both SINR and BER subplots.

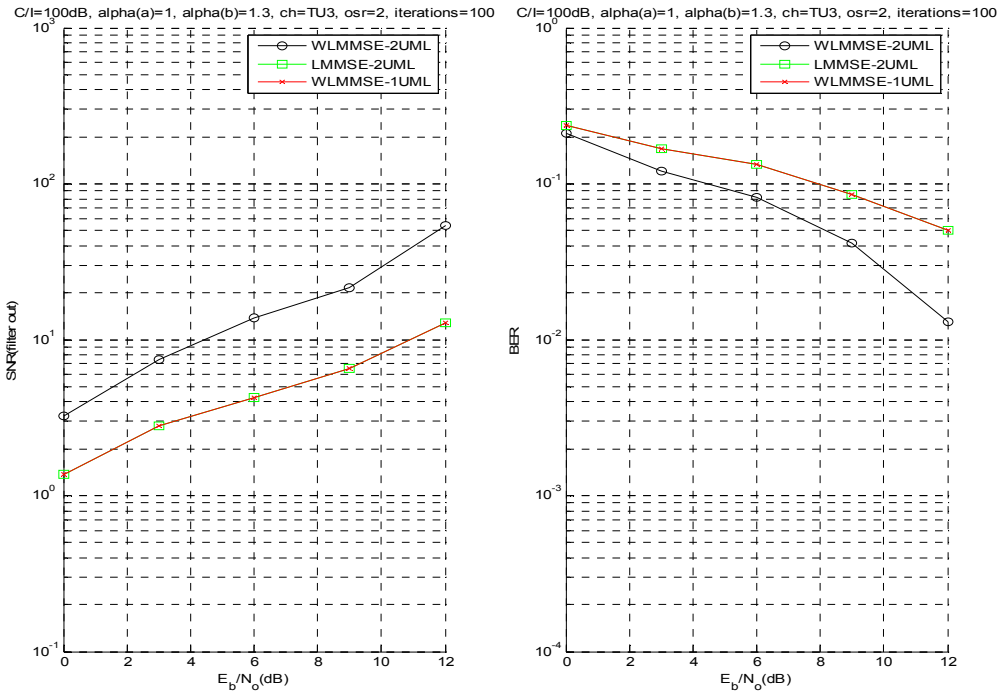


**Figure 5.5 Equalizer performance in the noise-limited test scenario with α=1**

### 5.2.4 Performance in the noise-limited test scenario with α=1.3

Since the transmitted signal is improper in this scenario, we expect WLMMSE-2UML performs the best. What is of interest is the performance gain of WLMMSE-2UML w.r.t. other equalizers and whether LMMSE-2UML is better than WLMMSE-1UML. In terms of BER performance, the figure below shows that WLMMSE-2UML is 0.5-1 dB better than LMMSE-2UML, and LMMSE-2UML is 2-2.5 dB better than WLMMSE-1UML.

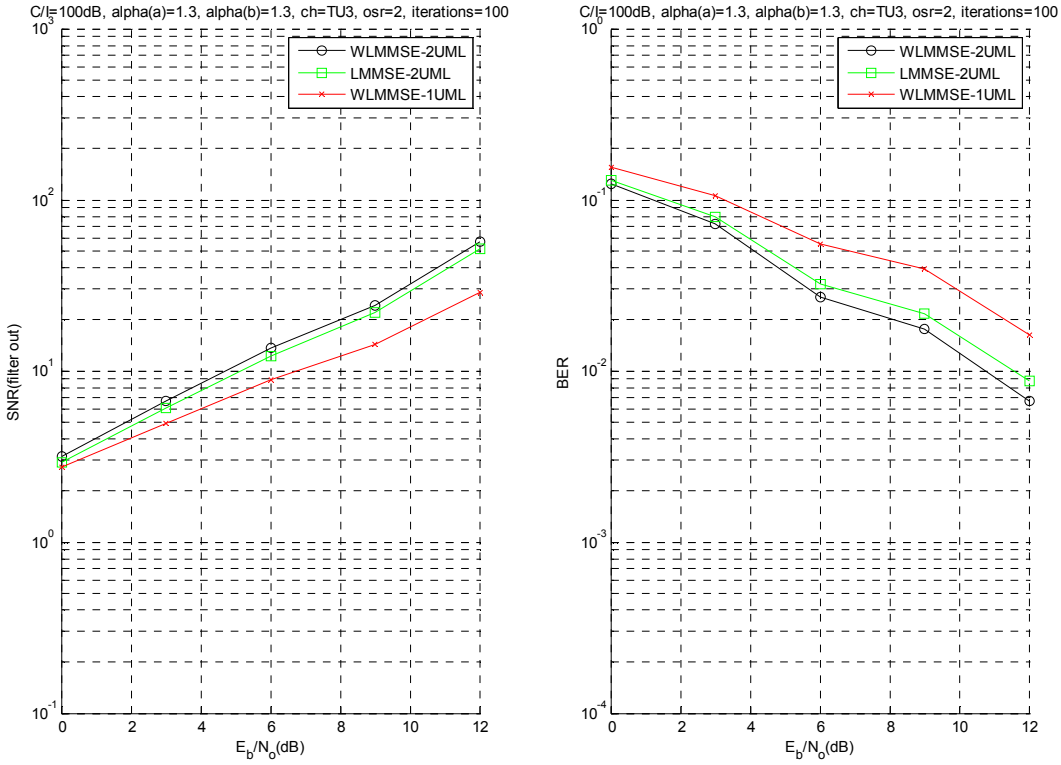


**Figure 5.6 Equalizer performance in the noise-limited test scenario with α=1.3**

### 5.2.5 Performance in the noise-limited test scenario with α=0.54

This test scenario provides some new information. Specifically, simulation results below shows that WLMMSE-2UML performs 2 dB worse than LMMSE-2UML, although its filter output SNR is better than that of LMMSE-2UML. This is not surprising because the widely linear filter allocates more power to the stronger user in order to yield a larger output SINR (both the desired user and the paired user are deemed as wanted signals from the filter's perspective; when α=0.54, the paired user is much stronger than the desired user).

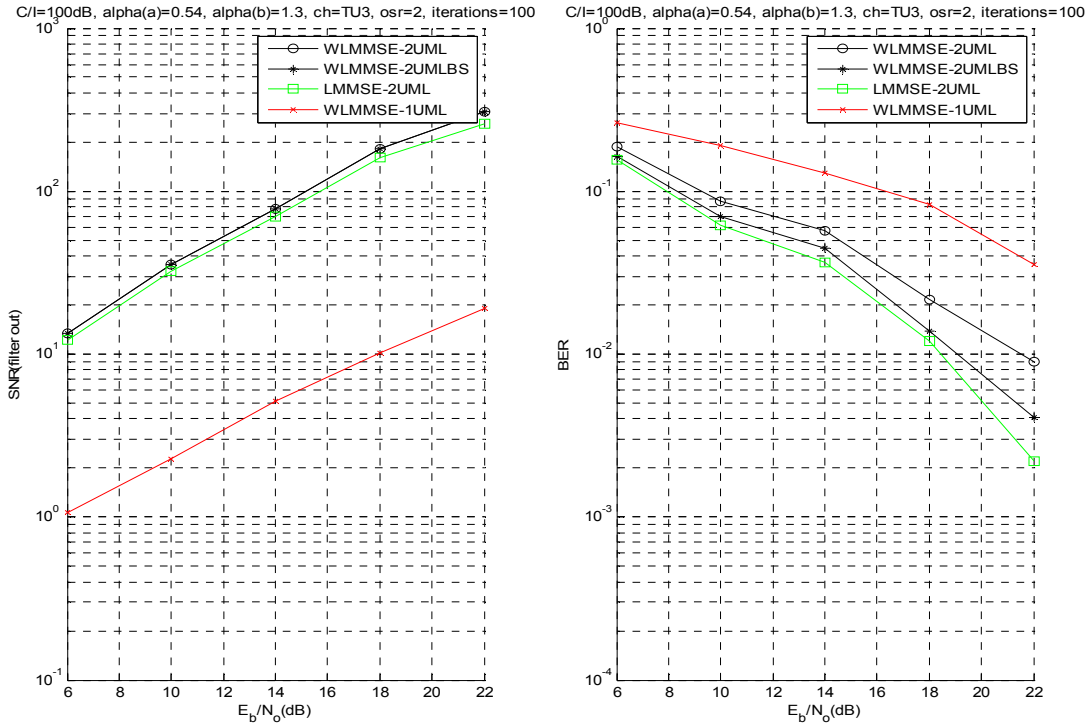


**Figure 5.7 Equalizer performance in the noise-limited test scenario with α=0.54**

There are several solutions to overcome this undesired situation. One obvious solution is to switch to LMMSE-2UML when α is less than 1. Here we apply a bootstrap method inspired by [1]. This equalizer performs the same filtering and JMLSE processing as WLMMSE-2UML in the first step. Then, as a threshold, if the energy of the paired user in the resulting post-filter CIR is greater than that of the desired user, BER of the paired user's detected sequence is expected to be lower than that of the desired user. In this case, contribution of the paired user to the received samples is reconstructed based on the paired user's detected sequence and estimated CIR, and removed from the received samples. Single-user equalization w.r.t. the desired user is followed to detect the desired user's sequence. Simulation shows that this solution is 1.5 dB better than WLMMSE-2UML but still 0.5 dB worse than LMMSE-2UML.

### 5.2.6 Performance in the interference-limited test scenario with user α=1 & interferer α=1

Since the transmitted signal and the received signal are jointly proper in this scenario, WLMMSE-2UML and LMMSE-2UML perform equally well and WLMMSE-1UML is the worst. We see that at 0.1 BER level, WLMMSE-1UML is only 0.5 dB worse; while at 0.05 BER level, WLMMSE-1UML becomes 2 dB worse. With increasing input C/I level, the WLMMSE-1UML curve further diverges from the WLMMSE-2UML and LMMSE-2UML curves. We may explain this result that when input SINR is low, JMLSE is not effective in interference cancellation because with high probability the received sample sequence is closer (in terms of Euclidean distance) to an valid but incorrect transmitted sequence; when input SINR is high, JMLSE becomes effective to detect the true transmitted sequence because with high probability the received sample sequence is closer to the correct transmitted sequence.

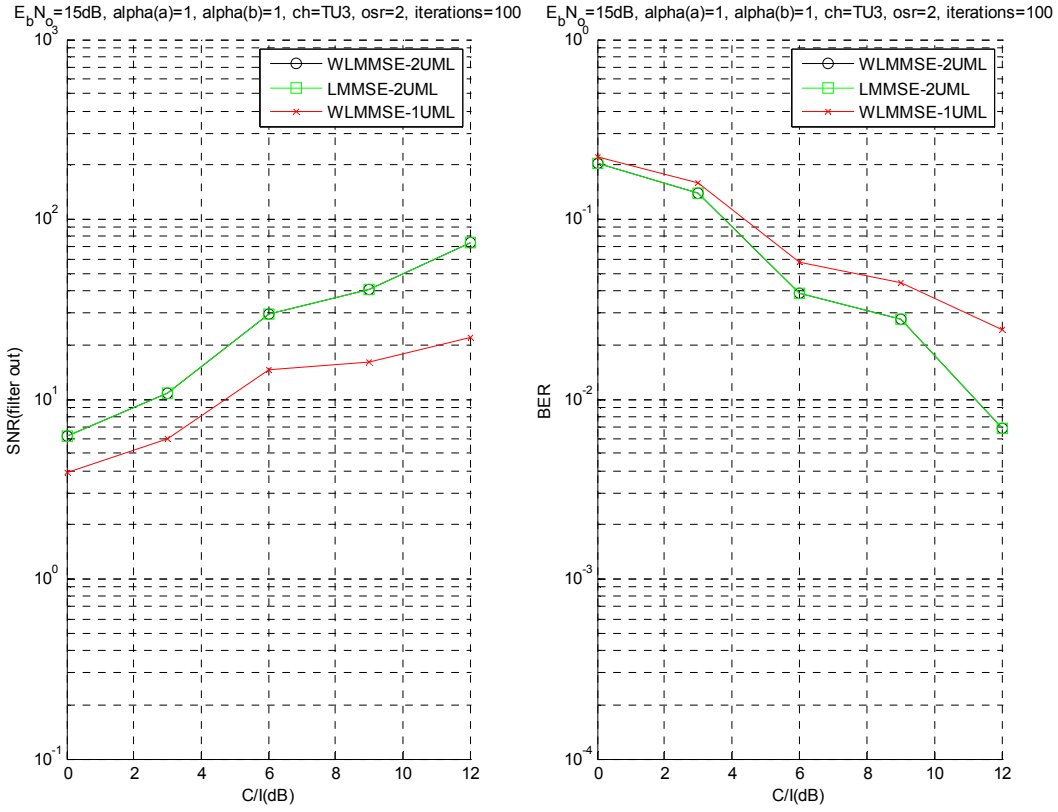


**Figure 5.8 Equalizer performance in the interference-limited test scenario with user α=1 & interferer α=1**

### 5.2.7 Performance in the interference-limited test scenario with user α=1.3 & interferer α=1

Since the transmitted signal is improper, WLMMSE-2UML performs better than LMMSE-2UML in this test scenario.

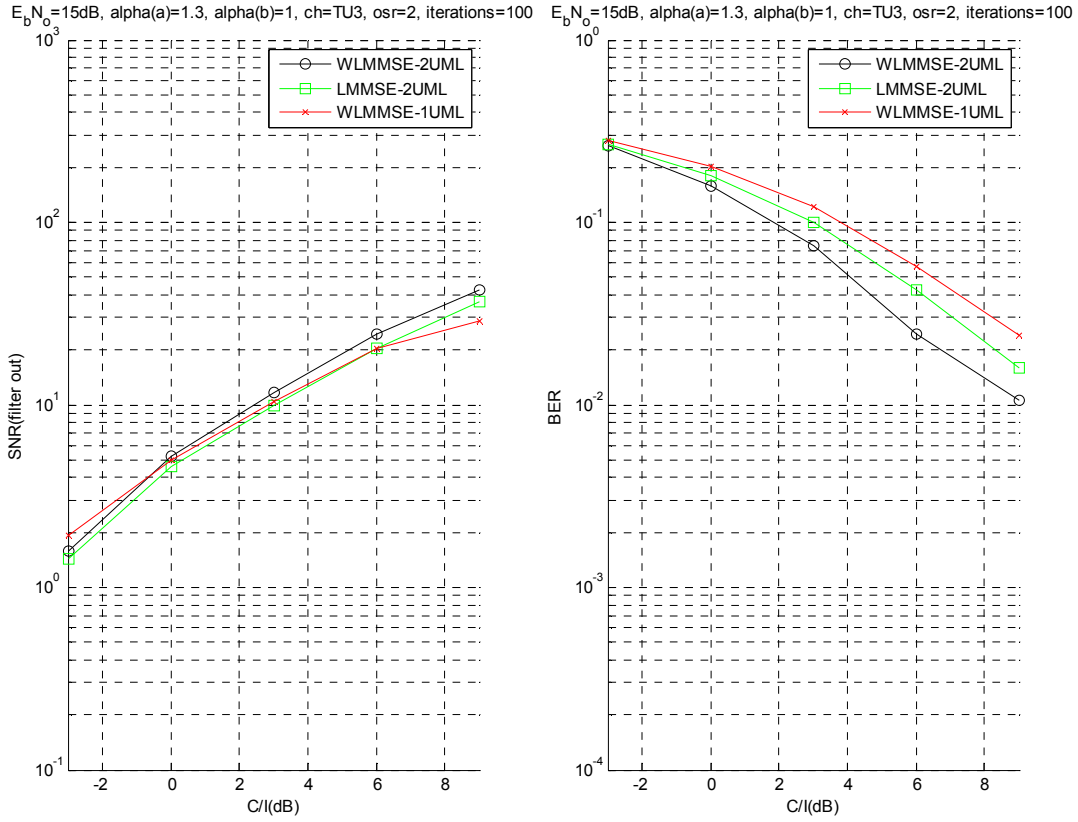


**Figure 5.9 Equalizer performance in the interference-limited test scenario with user α=1.3 & interferer α=1**

From the figure, the performance gain is 1-2 dB in the interested BER range. Meanwhile, we see that WLMMSE-1UML, although still the worst among the three equalizers, is only 1 dB less than LMMSE-2UML.

### 5.2.8 Performance in the interference-limited test scenario with user α=0.54 & interferer α=1

In this scenario, like the α=0.54 noise-limited test scenario in subsection 5.2.5, WLMMSE-2UML performs worse than LMMSE-2UML, and even worse than LMMSE-1UML in the low C/I region. By applying the bootstrap method, WLMMSE-2UMLBS brings the performance very close to LMMSE-2UML. It is worth further investigation to find a finer solution to make WLMMSE-2UML performs better than or at least equal to LMMSE-2UML in this test scenario.

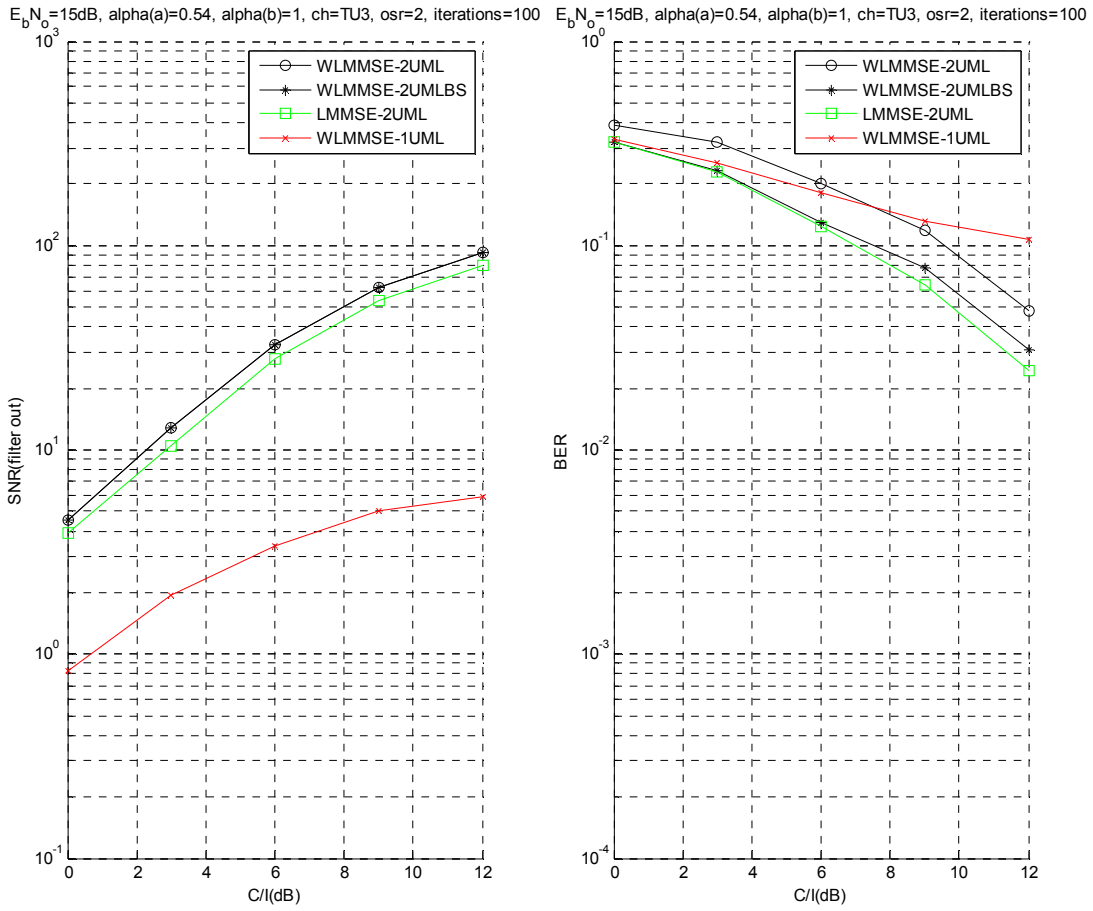


**Figure 5.10 Equalizer performance in the interference-limited test scenario with user α=0.54 & interferer α=1**

### 5.2.9 Performance in the interference-limited test scenario with user α=1.3 & interferer α=1.3

This may be the most suitable scenario to demonstrate the gain of WLP, because both user signal and the interference are improper. As expected, WLMMSE-2UML performs better than LMMSE-2UML, especially in the low C/I region. At 0.1 BER level, WLMMSE-2UML is 1.5 dB better than LMMSE-2UML; At 0.05 BER level, WLMMSE-2UML is 1.2 dB better than LMMSE-2UML; At 0.01 BER level, WLMMSE-2UML is 1 dB better than LMMSE-2UML. It is also observed that in this test scenario WLMMSE-1UML error performance approaches LMMSE-2UML in most C/I test region; this also justifies the value of WLP. For example, at 0.1 BER level, WLMMSE-1UML performs almost as well as LMMSE-2UML; at 0.05 BER level, WLMMSE-1UML is 0.5 dB worse than LMMSE-2UML.

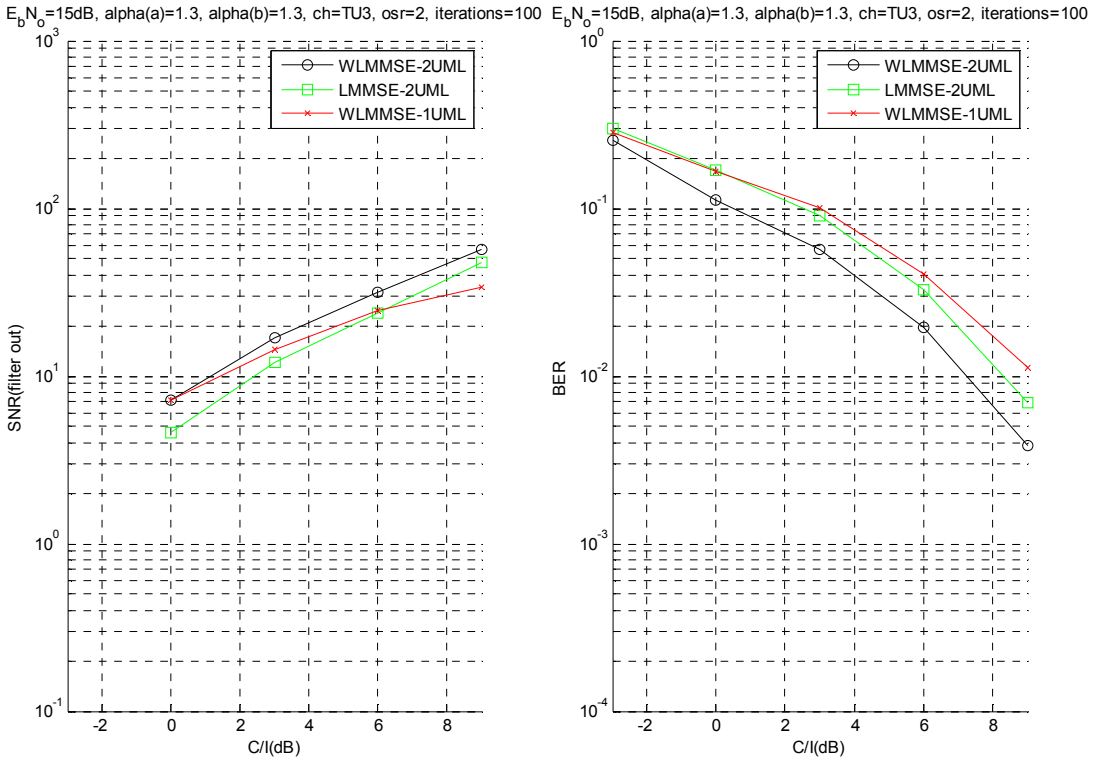


**Figure 5.11 Equalizer performance in the interference-limited test scenario with user α=1.3 & interferer α=1.3**

# Chapter 6
# Conclusions and further study

A novel equalizer consisting of a reduced rank widely linear MIMO MMSE filter and JMLSE is proposed in this work. Most of the novelty lies in the filter design, which jointly optimizes the MIMO MMSE filter coefficients matrix and the post-filter TIR matrix to minimize the filter output MSE with some constraint (in order to avoid trivial solutions such as all-zero coefficients). The ONC constraint from [37] is selected to constrain the the row vectors of the resulting post-filter TIR matrix to be orthonormal vectors. In order to optimize the overall equalizer BER performance, a TIR correction and noise balance unit is placed between the ONC-based MMSE filter and the JMLSE. Based on theoretical analysis in section 4.2, the cascade of these components makes the proposed equalizer equivalent to the noise whitening filter based equalizer in the rank-r channel matrix case. Since the solution is applicable to any channel matrix rank r between one (corresponding to the rank-one channel matrix) and min(M,N) (corresponding to the full-rank channel matrix), a generalized and scalable solution is obtained.

The equalizer is implemented in Matlab code and tested in various VAMOS test scenarios. Simulation results in chapter 5 confirm the equivalence between this MMSE based equalizer and noise whitening filter based equalizer in the known second order statistics case. When second order statistics have to be estimated, in general MMSE filter is more robust than noise whitening filter. The reason is that MMSE filter coefficients are calculated based on autocovariance of the received samples but noise whitening filter coefficients are calculated based on autocovariance of the noise sample vector which cannot be directly estimated, as we have discussed in previous chapters. Other simulation plots demonstrate that the proposed equalizer is better than some other equalizers in many typical VAMOS test scenarios. The only outstanding issue is that when the downlink transmission power in the desired user's subchannel is less than that of the other channel, the proposed widely linear MMSE filter and JMLSE equalizer yields worse BER performance than its linear filter based counterpart (but it is still better than the single-user MLSE based equalizer), although the filter output SINR of the widely linear filter is better than that of the linear filter. The reason is believed to be that the widely linear filter preserves more energy for the stronger user in order to maximize the output SINR (both the desired user and the paired user are deemed as wanted signals from the filter's perspective). A bootstrap solution based on [1] with a decent threshold is able to make the widely

linear filter based equalizer perform almost as well as its linear filter based counterpart in this particular test scenario.

Throughout this work, there are some unclear issues worth further investigation.

The first one is to find a more elegant method to optimize the proposed equalizer when the transmission power of the desired user's subchannel is less than that of the other subchannel. The bootstrap solution is computation intensive and it only brings the performance close to the linear filter based JMLSE equalizer.

The second issue is related to computation complexity of the equalizer. The full length JMLSE is used in our approach because the focus is the equalizer BER performance. The length of post-filter CIR is selected to be 5 symbol periods, because the true CIR ranging from transmitter to receiver spans 4 symbol periods and the space-time data model extends the post filter CIR by one more symbol period. This is sufficient in typical urban propagation model and the resulting computation load is manageable. Application of the equalizer in longer CIR cases or for a low-cost mobile station would require integration of a channel shortening or minimum phase filter to reduce the computation complexity (or more accurately, the number of trellis states) in the JMLSE stage.

We did not investigate equalizers with two physical antennas. Presumably mobile stations equipped with two physical antennas would be very effective in cancelling the interference in spatial domain. In that case, it may be worth looking into the performance differences with different combinations of oversampling, space-time data mode, widely linear processing, and antenna-array techniques.

# References


[1] C. Tidestav, M. Sternad and A. Ahlen, "Reuse within a cell-interference rejection or multiuser detection?" *Communications, IEEE Transactions on,* vol. 47, pp. 1511-1522, 1999.

[2] A. Mostafa, R. Kobylinski, I. Kostanic and M. Austin, "Single antenna interference cancellation (SAIC) for GSM networks," in *Vehicular Technology Conference, 2003. VTC 2003-Fall. 2003 IEEE 58th,* 2003, pp. 1089-1093 Vol.2.

[3] 3GPP, "3GPP TR 45.914, circuit switched voice capacity evolution for GSM/EDGE radio access network," 2009.

[4] F. D. Neeser and J. L. Massey, "Proper complex random processes with applications to information theory," *Information Theory, IEEE Transactions on,* vol. 39, pp. 1293-1302, 1993.

[5] B. Picinbono and P. Chevalier, "Widely linear estimation with complex data," *Signal Processing, IEEE Transactions on,* vol. 43, pp. 2030-2033, 1995.

[6] P. J. Schreier and L. L. Scharf, "Second-order analysis of improper complex random vectors and processes," *Signal Processing, IEEE Transactions on,* vol. 51, pp. 714-725, 2003.

[7] P. Jung, "Laurent's representation of binary digital continuous phase modulated signals with modulation index 1/2 revisited," *Communications, IEEE Transactions on,* vol. 42, pp. 221-224, 1994.

[8] Jen-Wei Liang, Jiunn-Tsair Chen and A. J. Paulraj, "A two-stage hybrid approach for CCI/ISI reduction with space-time processing," *Communications Letters, IEEE,* vol. 1, pp. 163-165, 1997.

[9] F. Pipon, P. Chevalier, P. Vila and J. -. Monot, "Joint spatial and temporal equalization for channels with ISI and CCI-theoretical and experimental results for a base station reception," in *Signal Processing Advances in Wireless Communications, 1997 First IEEE Signal Processing Workshop on,* 1997, pp. 309-312.

[10] P. A. Hoeher, S. Badri-Hoeher, Shiyang Deng, C. Krakowski and Wen Xu, "Single antenna interference cancellation (SAIC) for cellular TDMA networks by means of joint delayed-decision feedback sequence estimation," *Wireless Communications, IEEE Transactions on,* vol. 5, pp. 1234-1237, 2006.

[11] D. Hui and A. Hafeez, "Effective interference suppression via spatio-temporal block decorrelation," in *Personal, Indoor and Mobile Radio Communications, 2007. PIMRC 2007. IEEE 18th International Symposium on,* 2007, pp. 1-5.

[12] R. Meyer, W. H. Gerstacker, R. Schober and J. B. Huber, "A single antenna interference cancellation algorithm for increased gsm capacity," *Wireless Communications, IEEE Transactions on,* vol. 5, pp. 1616-1621, 2006.

[13] J. C. Olivier and W. Kleynhans, "Single antenna interference cancellation for synchronised GSM networks using a widely linear receiver," *Communications, IET,* vol. 1, pp. 131-136, 2007.

[14] G. Forney Jr., "Maximum-likelihood sequence estimation of digital sequences in the presence of intersymbol interference," *Information Theory, IEEE Transactions on,* vol. 18, pp. 363-378, 1972.

[15] M. V. Eyuboglu and S. U. H. Qureshi, "Reduced-state sequence estimation with set partitioning and decision feedback," *Communications, IEEE Transactions on,* vol. 36, pp. 13-20, 1988.

[16] W. van Etten, "Maximum Likelihood Receiver for Multiple Channel Transmission Systems," *Communications, IEEE Transactions on,* vol. 24, pp. 276-283, 1976.

[17] P. A. Ranta, A. Hottinen and Z. -. Honkasalo, "Co-channel interference cancelling receiver for TDMA mobile systems," in *Communications, 1995. ICC '95 Seattle, 'Gateway to Globalization', 1995 IEEE International Conference on,* 1995, pp. 17-21 vol.1.

[18] A. Hafeez, R. Ramesh and D. Hui, "Maximum SNR prefiltering for MIMO systems," in *Signal Processing Advances in Wireless Communications, 2005 IEEE 6th Workshop on,* 2005, pp. 186-190.

[19] W. H. Gerstacker, P. Nickel and D. P. Taylor, "Diversity interference cancellation using prefiltering and reduced-state MIMO equalization," in *Acoustics, Speech, and Signal Processing, 2004. Proceedings. (ICASSP '04). IEEE International Conference on,* 2004, pp. iv-813-16 vol.4.

[20] Telefon AB LM Ericsson, "3GPP tdoc GP-090224, SAM - single antenna MIMO - for VAMOS," in 3GPP TSG GERAN #41, St Julians, Malta, 2009.

[21] D. Asztely and B. Ottersten, "MLSE and spatio-temporal interference rejection combining with antenna arrays," in Ninth European Signal Processing Conference Eusipco-98, 1998.

[22] W. van Etten, "An Optimum Linear Receiver for Multiple Channel Digital Transmission Systems," *Communications, IEEE Transactions on,* vol. 23, pp. 828-834, 1975.

[23] 3GPP, "3GPP TS 45.002, multiplexing and multiple access on the radio path," 2009.

[24] N. Khouja, K. Grati, A. Ghazel and B. Le Gal, "Design and implementation of a reconfigurable decimation and channel selection filter for GSM and UMTS radio standards," in *Wireless Communications and Networking Conference, 2009. WCNC 2009. IEEE,* 2009, pp. 1-6.

[25] 3GPP, "3GPP TS 45.005, radio transmission and reception," 2009.

[26] G. L. Stüber, *Principles of Mobile Communication (2nd Edition)* Springer, 1996.

[27] D. T. M. Slock and C. B. Papadias, "Blind fractionally-spaced equalization based on cyclostationarity," in *Vehicular Technology Conference, 1994 IEEE 44th,* 1994, pp. 1286-1290 vol.2.

[28] B. Widrow, P. E. Mantey, L. J. Griffiths and B. B. Goode, "Adaptive antenna systems," *Proceedings of the IEEE,* vol. 55, pp. 2143-2159, 1967.

[29] S. Applebaum, "Adaptive arrays," *Antennas and Propagation, IEEE Transactions on,* vol. 24, pp. 585-598, 1976.

[30] M. Honig, U. Madhow and S. Verdu, "Blind adaptive multiuser detection," *Information Theory, IEEE Transactions on,* vol. 41, pp. 944-960, 1995.

[31] P. J. W. Melsa, R. C. Younce and C. E. Rohrs, "Impulse response shortening for discrete multitone transceivers," *Communications, IEEE Transactions on,* vol. 44, pp. 1662-1672, 1996.

[32] N. Al-Dhahir and J. M. Cioffi, "MMSE decision-feedback equalizers: finite-length results," *Information Theory, IEEE Transactions on,* vol. 41, pp. 961-975, 1995.

[33] E. Lindskog and C. Tidestav, "Reduced rank space-time equalization," in *Personal, Indoor and Mobile Radio Communications, 1998. the Ninth IEEE International Symposium on,* 1998, pp. 1081-1085 vol.3.

[34] G. Ungerboeck, "Adaptive Maximum-Likelihood Receiver for Carrier-Modulated Data-Transmission Systems," *Communications, IEEE Transactions on,* vol. 22, pp. 624-636, 1974.

[35] R. Ramesh, D. Hui, A. -. Hafeez and H. Arslan, "Prefilter design for low-complexity equalization of MIMO systems," in *Vehicular Technology Conference, 2004. VTC 2004-Spring. 2004 IEEE 59th,* 2004, pp. 871-875 Vol.2.

[36] Yingbo Hua, M. Nikpour and P. Stoica, "Optimal reduced-rank estimation and filtering," *Signal Processing, IEEE Transactions on,* vol. 49, pp. 457-469, 2001.

[37] N. Al-Dhahir, "FIR channel-shortening equalizers for MIMO ISI channels," *Communications, IEEE Transactions on,* vol. 49, pp. 213-218, 2001.

[38] K. Kuchi and V. K. Prabhu, "Interference cancellation enhancement through generalized widely linear equalization in QAM systems," *Wireless Communications, IEEE Transactions on,* vol. 8, pp. 1585-1590, 2009.

[39] J. M. Cioffi, G. P. Dudevoir, M. Vedat Eyuboglu and G. D. Forney Jr., "MMSE decision-feedback equalizers and coding. I. Equalization results," *Communications, IEEE Transactions on,* vol. 43, pp. 2582-2594, 1995.

[40] N. Al-Dhahir and A. H. Sayed, "The finite-length multi-input multi-output MMSE-DFE," *Signal Processing, IEEE Transactions on,* vol. 48, pp. 2921-2936, 2000.

[41] R. A. Horn and C. R. Johnson, *Topics in Matrix Analysis* Cambridge University Press, 1994.

[42] R. Meyer, W. H. Gerstacker, F. Obernosterer, M. A. Ruder and R. Schober, "Efficient receivers for GSM MUROS downlink transmission," in *Personal, Indoor and Mobile Radio Communications, 2009 IEEE 20th International Symposium on,* 2009, pp. 2399-2403.

[43] Nokia Corp, "3GPP tdoc GP-090320, performance of DARP phase 1 and VAMOS aware terminals," in 3GPP TSG GERAN #41, St Julians, Malta, 2009.